



Changes in ambient air quality and atmospheric composition and reactivity in the South East of the UK as a result of the COVID-19 lockdown



K.P. Wyche^{a,*}, M. Nichols^b, H. Parfitt^c, P. Beckett^c, D.J. Gregg^a, K.L. Smallbone^a, P.S. Monks^d

^a Air Environment Research, University of Brighton, Lewes Road, Brighton BN2 4GJ, UK

^b Hydrock Consultants Ltd, Merchants House North, Wapping Road, Bristol BS1 4RW, UK

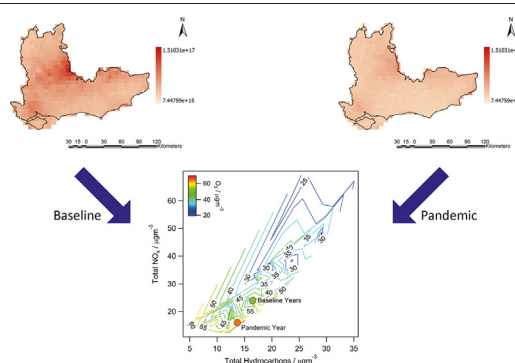
^c Phlorum Ltd, 12 Hunns Mere Way, Brighton BN2 6AH, UK

^d Department of Chemistry, University of Leicester, University Road, Leicester LE1 7RH, UK

HIGHLIGHTS

- Boundary layer trace composition changed during the COVID-19 pandemic.
- NO₂ concentrations across measurement sites were down by ~14–38%.
- PM₁₀/PM_{2.5} concentrations were influenced by interregional pollution episodes.
- O₃ concentrations were up by as much as 15% and total O_x levels were ~ preserved.
- Under HC limited regime, increased O₃ led to increased radicals and reactivity.

GRAPHICAL ABSTRACT



ARTICLE INFO

Article history:

Received 20 July 2020

Received in revised form 14 September 2020

Accepted 17 September 2020

Available online 24 September 2020

Editor: Lidia Morawska

Keywords:

Anthropause

Coronavirus

Lockdown

Nitrogen dioxide

Ozone

Oxidative capacity

ABSTRACT

The COVID-19 pandemic forced governments around the world to impose restrictions on daily life to prevent the spread of the virus. This resulted in unprecedented reductions in anthropogenic activity, and reduced emissions of certain air pollutants, namely oxides of nitrogen. The UK 'lockdown' was enforced on 23/03/2020, which led to restrictions on movement, social interaction, and 'non-essential' businesses and services. This study employed an ensemble of measurement and modelling techniques to investigate changes in air quality, atmospheric composition and boundary layer reactivity in the South East of the UK post-lockdown. The techniques employed included *in-situ* gas- and particle-phase monitoring within central and local authority air quality monitoring networks, remote sensing by long path Differential Optical Absorption Spectroscopy and Sentinel-5P's TROPOMI, and detailed 0-D chemical box modelling. Findings showed that de-trended NO₂ concentrations decreased by an average of 14–38% when compared to the mean of the same period over the preceding 5-years. We found that de-trended particulate matter concentrations had been influenced by interregional pollution episodes, and de-trended ozone concentrations had increased across most sites, by up to 15%, such that total O_x levels were roughly preserved. 0-D chemical box model simulations showed the observed increases in ozone concentrations during lockdown under the hydrocarbon-limited ozone production regime, where total NO_x decreased proportionally greater than total non-methane hydrocarbons, which led to an increase in total hydroxyl, peroxy and organic peroxy radicals. These findings suggest a more complex scenario in terms of changes in air

* Corresponding author at: Air Environment Research, School of Environment and Technology, University of Brighton, Brighton BN2 4GJ, UK.
E-mail address: k.p.wyche@brighton.ac.uk (K.P. Wyche).

quality owing to the COVID-19 lockdown than originally reported and provide a window into the future to illustrate potential outcomes of policy interventions seeking large-scale NO_x emissions reductions without due consideration of other reactive trace species.

© 2020 The Authors. Published by Elsevier B.V. This is an open access article under the CC BY-NC-ND license (<http://creativecommons.org/licenses/by-nc-nd/4.0/>).

1. Introduction

By the 1st July 2020 there were in excess of 10 million confirmed cases of COVID-19 worldwide. Of these cases, it was reported that the virus had claimed an estimated 511,037 lives (ECDC, 2020). In an effort to halt the spread of the disease, governments across the globe put into place a range of measures based on 'social distancing' and 'self-isolation', which resulted in many industries suspending operations and most citizens (*i.e.* non 'key-workers') staying in their homes (PHE, 2020a). As such, anthropogenic activity around the globe decreased rapidly, to such an extent that emissions of air pollutants began to decline dramatically, with this period now being referred to as an 'anthropause' (Rutz et al., 2020). In the early stages of the pandemic, remote sensing data from satellites indicated that nitrogen dioxide (NO₂) concentrations had fallen by as much as 30% across China and by as much as 50% across areas of central Europe (NASA, 2020). Early work using *in-situ* measurements confirmed these findings, with studies from China (Chen et al., 2020), Korea (Ju et al., 2020), India (Sharma et al., 2020), USA (Zangari et al., 2020) and Europe (Tobías et al., 2020; Sicard et al., 2020) all reporting decreases in ambient NO_x concentrations. The UK government advised that the general population should avoid 'non-essential' travel and social contact, on 16th March 2020. At this point, the total number of confirmed cases in the UK had surpassed 1500. Subsequently, on 23rd March 2020, the government announced a UK-wide partial 'lockdown', to contain the spread of the virus. The Health Protection (Coronavirus, Restrictions) (England) Regulations 2020 (SI 350) (PHE, 2020b), the statutory instrument to enforce the lockdown, was enacted shortly after. The total number of confirmed COVID-19 cases and deaths in the UK from 1st January 2020 to 6th July 2020, is shown in the Supplementary material (Fig. S1), for reference.

Air pollution is one of the single biggest on-going threats facing global public health today (WHO, 2016). It is estimated that ~90% of the world's population live in areas where levels of air pollution are above limits deemed safe for human health (WHO, 2018), and that this results in ~7-million deaths per year (*i.e.* ~13% of all global deaths) and a reduction in average life expectancy by ~2-years (Greenstone and Fan, 2018). Consequently, it follows that such a significant and widespread reduction in air pollutant emissions as has been experienced across the globe during the COVID-19 pandemic, should result in a decrease in air pollution related morbidity and mortality. According to recent research by the Centre for Research on Energy and Clean Air, the reductions in NO₂ and particulate matter (PM) experienced across Europe after government restrictions were put into place was likely to have reduced the number of air pollution associated deaths by 11,000 over just 30 days (Myllyvirta and Thieriot, 2020). However, such estimates do not take into account changes in the abundance of secondary pollutants, which can often be proportionally more harmful to human health than some primary species (*e.g.* Mustafa et al., 1984).

Such a dramatic reduction in certain air pollutants across the species emissions spectrum, over such a relatively short time interval and across so many different countries, is unprecedented. As such, the resultant impacts on tropospheric chemical processes and composition need to be investigated. For instance, with reductions in ambient NO_x (*i.e.* NO + NO₂) concentrations there will be a shift in the balance of chemistry, and levels of secondary pollutants such as ozone (O₃) are likely to be perturbed from the expected norm (Monks et al., 2015). Also, we are likely to experience a shift in the size distribution of particulate numbers; as PM_{2.5} and PM₁₀ act to suppress the formation and abundance

of ultrafine particles (UFP; Guo et al., 2020). A reduction in the abundance of larger particles could result in a burst in the number concentration of the finest, more harmful fractions (*e.g.* Harrison and Yin, 2000; Araujo and Nel, 2009; Ruckerl et al., 2011; Hofman et al., 2016; Rychlik et al., 2019).

Therefore, it is vital that we act rapidly to quantify and understand the changes occurring within our atmosphere, particularly with respect to major respiratory air pollutants which can exacerbate the effects of respiratory diseases such as COVID-19, and pollutants which could act as vectors for these viruses (Comunian et al., 2020). One major tool available to assist in this regard is the network of automated air pollution monitors installed by central governments to make the necessary measurements of air pollution parameters to check air quality levels and ensure regulatory compliance (Munn, 1981). In the UK, the national *Automatic Urban and Rural Network* (AURN) is run by the *Environment Agency* on behalf of the UK Government *Department for Food and Rural Affairs* (DEFRA). It currently comprises 150 monitoring stations deployed in a range of different receptor environments (DEFRA, 2020a), supported by various local authority networks, including in the South East of the UK, *The Sussex-Air Network* (SUSSEX-AIR, 2020).

In this work, we combine findings from the AURN and Sussex-Air Network with data from the University of Brighton *JOAQUIN Advanced Air Quality reSearch* (JAAQS) laboratory and ESA's *Sentinel-5P* satellite, to investigate changes in tropospheric composition and reactivity in the South East of the UK during the COVID-19 pandemic. The South East of the UK is an interesting region for studying air quality, having the largest regional population of the country, with an estimated 9.13 million people living in the area according to the latest available census data published by the Office for National Statistics (ONS, 2020), and being geographically located between two major air pollution hotspots, *i.e.* the mega-city of London and the industrial and urbanised North West Europe. The results presented show a more complex scenario with respect to atmospheric reactivity than has been initially reported, with falling NO₂ concentrations, interregional particulate matter episodes and rising O₃ levels (particularly under urban conditions). Unlike other studies conducted thus far, we integrate comprehensive air quality measurements made both *in-situ* and by remote sensing with non-methane hydrocarbon (NMHC) data and near-explicit 0D chemical box modelling to investigate perturbations to chemical processes. Our findings show that the abundance of NMHCs in the suburban boundary layer (of outer London in the South East of the UK) decreased proportionally less than total NO_x species, such that there was an increase in the NMHC:NO_x ratio and a resultant shift within the NMHC sensitive regime toward greater net O₃ production. Model simulations indicate that these perturbations to local boundary layer air led to an increase in hydroxyl radical (OH) concentrations and a potential change in oxidative capacity/capability.

2. Methodology

2.1. The Automatic Urban and Rural Network and Sussex-Air Network

Twenty-five automatic monitoring stations, including six Automatic Urban and Rural Network (AURN) stations, seventeen Sussex-Air and two monitoring stations managed by the Transport Research Laboratory (TRL), with appropriate data coverage, were available in the study area. The locations of these sites are shown in Fig. S2 in the Supplementary material and further information, including environment type and

Table 1
Automatic monitoring site parameters and site codes.

Code	Site name	Environment	Coordinates	Instruments ^a
AD1	Shoreham High Street	Kerbside	50.832173, -0.277498	CL-NO _x , BAM-PM10
AR1	Chichester Lodsworth	Rural Background	51.001180, -0.684602	UVA-O ₃
AR2	Wealden Isfield	Rural Background	50.938397, 0.060765	UVA-O ₃
BH0	Brighton Preston Park	Urban Background	50.840836, 0.147572	CL-NO _x , UVA-O ₃ , TEOM-PM _{2.5}
BH4	Brighton North Street	Kerbside	50.823203, -0.141525	CL-NO _x , TEOM-PM ₁₀
BH6	Brighton Lewes Road	Kerbside	50.835708, -0.125606	CL-NO _x , TEOM-PM ₁₀
CA2	Gatwick East	Urban Background	51.157645, -0.151071	CL-NO _x , FDAS-PM ₁₀ , FDAS-PM _{2.5}
CI1	Chichester A27 Chichester Bypass	Kerbside	50.827304, -0.782009	CL-NO _x , TEOM-PM ₁₀
CI4	Chichester Orchard Street	Kerbside	50.840130, -0.780289	CL-NO _x
CI5	Chichester Westhampnett Road	Kerbside	50.841297, -0.762746	TEOM-PM ₁₀
EB1	Eastbourne Devonshire Park	Urban Background	50.762450, 0.284044	CL-NO _x , UVA-O ₃ , BAM-PM10
EB3	Eastbourne Holly Place	Urban Background	50.805810, 0.271610	FDAS-PM ₁₀ , FDAS-PM _{2.5}
FAL	Brighton University Falmer ^b	Suburban Background	50.860317, 0.088056	DOAS, Weather station
HO2	Horsham Parkway	Kerbside	51.062618, -0.324817	CL-NO _x , TEOM-PM ₁₀
HO4	Horsham Storrington	Kerbside	50.917421, -0.450878	CL-NO _x , TEOM-PM ₁₀ , TEOM-PM _{2.5}
HOT (HO5)	Horsham Cowfold	Kerbside	50.989087, -0.270257	CL-NO _x
HT1	Hastings Bulverhythe	Kerbside	50.850777, 0.522117	CL-NO _x , TEOM-PM ₁₀
LL1	Wealden Lullington Heath	Rural Background	50.793566, 0.180838	CL-NO _x , UVA-O ₃
LS5	Lewes West Street	Kerbside	50.874388, 0.010355	CL-NO _x , UVA-O ₃ , TEOM-PM ₁₀
RG1	Horley Michael Crescent	Suburban Background	51.165884, -0.167734	CL-NO _x , TEOM-PM ₁₀ , Weather station
RG3	Crawley Poles Lane	Rural Background	51.141722, -0.194509	CL-NO _x , UVA-O ₃ , Weather station
RG5	Reigate and Banstead	Suburban Background	51.16583, -0.167764	TEOM-PM ₁₀
RG6	Horley The Crescent	Suburban Background	51.161261, -0.162410	CL-NO _x , TEOM-PM ₁₀
RG7	Hooley A23	Kerbside	51.292471, -0.154121	CL-NO _x
RY1	Rother Rye Harbour	Rural Background	50.939004, 0.766141	UVA-O ₃
RY2	Rother De La Warr Road	Kerbside	50.845402, 0.492920	CL-NO _x

^a CL-NO_x = chemiluminescence NO_x analyser; UVA-O₃ = UV absorption O₃ analyser; TEOM-PM_{2.5} = Tapered Element Oscillating Microbalance with Filter Dynamics Measurement System PM_{2.5} analyser; TEOM-PM₁₀ = Tapered Element Oscillating Microbalance with Filter Dynamics Measurement System PM₁₀ analyser; FDAS = Palas Fidas; DOAS = Differential Absorption Spectroscopy

^b See Methodology for instrument details.

pollutants monitored, are listed in Table 1. Each monitoring station was variably equipped with chemiluminescence NO_x, UV absorption O₃ and sulphur dioxide (SO₂) infrared absorption gas-phase analysers, and Fidas-200, Beta Attenuation Monitor (BAM), or Tapered Element Oscillating Microbalance with Filter Dynamics Measurement System (TEOM-FDMS) gravimetric PM analysers. All AURN and Sussex-Air Network data were screened for service periods and anomalies prior to analysis.

2.2. The JOAQUIN Advanced Air Quality reSearch Laboratory

The JOAQUIN Advanced Air Quality reSearch Laboratory (JAAQS) was established in Brighton in 2015. It comprises a climate controlled, clean laboratory instrumented with a suite of state-of-the-art analytical instruments for making detailed, *real-time* measurements of tropospheric composition. It is equipped with long-path Differential Optical Absorption Spectroscopy (DOAS; Opsis AB) for remote sensing of trace gas parameters (path length ~ 300 m), including NO₂, O₃, SO₂, formaldehyde (HCHO), nitrous acid (HONO) and benzene (C₆H₆; indicative data only); total and size-resolved particle counters ($7 \leq n \leq 1000$ nm; TSI 3031 and TSI 3783); a black carbon monitor (Thermo MAAP 5012); a PM_{2.5} monitor (Met One ES-642); and a meteorology station (Campbell Scientific; data from 01/01/2019). JAAQS is situated in a suburban background environment, roughly 5 km from Brighton city centre. JAAQS data were recorded at 5-minute averaging intervals and were screened for service periods and anomalies prior to analysis.

2.3. Meteorology data

Regional meteorology data were obtained from Shoreham Airport, Gatwick Airport, Herstmonceaux and Lydd, and local meteorology data were obtained from the JAAQS Laboratory in Brighton and Hove. Parameters employed, included wind speed (ms⁻¹), wind direction (°), atmospheric pressure (Pa), relative humidity (%), air temperature (°C) and solar radiation (Wm⁻²). South East regional meteorology data for Shoreham Airport, Gatwick Airport, Herstmonceaux and Lydd

were extracted from NOAA's Integrated Surface Database using the R Package 'worldmet' (Carslaw, 2020). Regional meteorology data were recorded at hourly averaging intervals, and local meteorology data were recorded at 10-minute averaging intervals; both data sets were screened for service periods and anomalies prior to analysis. Back trajectory analyses were conducted for key periods using the NOAA Hybrid Single Particle Lagrangian Integrated Trajectory (HYSPLIT) transport and dispersion model (<http://ready.arl.noaa.gov/HYSPLIT.php>).

2.4. Data analysis procedure

After all data sets were screened for errors, anomalies, instrument downtime and maintenance intervals, they were analysed using the open-source Openair tools (Carslaw, 2015) in the statistical computing software, R (R Development Core Team, 2015). Data capture percentage for 2015–2020, for each monitoring site used for analysis is provided in the Supplementary material (Table S1). As part of the analysis procedure, the 'de-weather' package within Openair was used to 'de-trend' the data and remove the influence of meteorology in order to help assess the extent to which changes in ambient pollutant concentrations were attributed to sudden changes in emissions following government-imposed lockdown restrictions (Grange and Carslaw, 2019). Each 'de-weather' analysis was conducted using historic 5-year air pollutant monitoring and regional meteorological data.

Further analytical methods were then applied to the de-weathered data, namely relative change analysis, and normalisation; key summary statistics are given in Table 2. To produce the data in Table 2, period mean data for March to May, inclusive, were calculated for all assessment years (*i.e.* 2015–2020). This enabled comparison of average de-weathered pollutant concentrations during lockdown with the preceding 5-year mean (*i.e.* 2015–2019) for the same period, both in terms of absolute and relative percentage changes. In addition, de-weathered data were normalised to the 2020 average to produce Fig. 1(a–d), and to the 2015–2019 annual averages to produce Fig. S3(a–d) to show

Table 2

Changes in period mean (*i.e.* March–May, inclusive) ‘de-weathered’ air pollutant concentrations in the South East of the UK between 2020 (during the pandemic) and the average of the same period over the preceding 5 years (*i.e.* 2015–2019). Summary statistics by site type are also provided.

Site	NO ₂		O ₃		PM ₁₀		PM _{2.5}	
	Absolute / $\mu\text{g m}^{-3}$	Relative / %						
Kerbside								
AD1	-17.5	51.2			-5.7	79.9		
BH4	-22.4	47.2			-4.6	69.5		
BH6	-67.0	17.7			-0.3	95.7		
CI1	-13.1	59.7			-1.8	90.9		
CI4	-7.5	67.3						
CI5					-2.0	90.5		
HO2	-7.4	72.3			-1.1	94.6		
HO4	-6.0	74.2						
HOT (HO5)	-5.4	80.2			-1.1	94.6		
HT1	-5.6	68.8			-3.1	87.6		
LS5	-6.4	70.1	7.0	112.1				
RG7	-15.1	68.1						
RY2	-7.6	65.7						
Mean	-15.1	61.9	7.0	112.1	-2.5	87.9		
Urban background								
BH0	-4.2	74.1	3.7	107.3			2.0	115.3
CA2	-15.0	43.9			-8.9	68.1	2.9	129.9
EB1	1.6	116.5	2.7	104.6	-5.0	78.6		
EB3	1.2	110.4						
EF1					-3.4	82.9	-3.9	73.9
Mean	-4.1	86.2	3.2	106.0	-5.8	76.5	0.3	106.4
Suburban background								
FAL	-8.4	63.6	8.5	115.2				
RG1	-7.9	61.0			-1.6	90.7		
RG5	-5.7	67.8			-2.0	87.6		
RG6	-11.0	57.5						
Mean	-8.3	62.5	8.5	115.2	-1.8	89.2		
Rural background								
LL1	-0.9	88.5	-5.5	90.6				
RG3	-4.8	67.9	6.2	112.1				
AR1			1.7	103.2				
AR2			-3.6	93.2				
RY1			2.9	105.2				
Mean	-2.9	78.2	0.3	100.9				
All site mean	-10.7	67.9	2.9	105.0	-3.1	85.5	0.3	106.4

Cell colour scale represents the level of change in concentration. The darker the shade of blue, the larger the reduction in concentration for that particular pollutant; lighter shades/white represent the middle of the change scale; the darker reds represent the opposite end of the scale, where concentrations have decreased the least or increased.

the deviation in average pollutant concentrations during 2020 from the preceding 5-year mean.

2.5. Sentinel-5P TROPOMI observations

Level-2 (L2) TROPOMI NO₂ products were sourced from the *Sentinel-5P Pre-Operations Data Hub* for dates between 23rd March and 22nd April of both 2019 and 2020 (Copernicus, 2020). The pixels covering the South East quadrant of the UK were extracted from each dataset and filtered to remove problematic and cloud influenced observations, *i.e.* where pixel values were negative or associated with a Quality Assurance flag <0.75 (Eskes et al., 2019). The filtered data were appropriately averaged, and units converted to molec cm⁻². Percentage changes in tropospheric column NO₂ values were determined by expressing the

concentration difference between 2020 and 2019 as a fraction of the 2019 value before multiplying by one hundred.

2.6. Model construction

The average diurnal evolution of local boundary layer gas-phase composition in the spring before (*i.e.* March, April and May over the period 2015–2019, inclusive) and after initiation of lockdown restrictions (*i.e.* from 24th March to 31st May 2020), was simulated using a 0-D photochemical box model incorporating appropriate inorganic and organic atmospheric oxidation schemes extracted from the Master Chemical Mechanism (v3.3.1; Jenkin et al., 1997; Jenkin et al., 2002; Saunders et al., 2003; <http://mcm.leeds.ac.uk/MCM>). With no comprehensive non-methane hydrocarbon (NMHC) data available in the monitoring networks of the South East of the UK, the data required to initialise

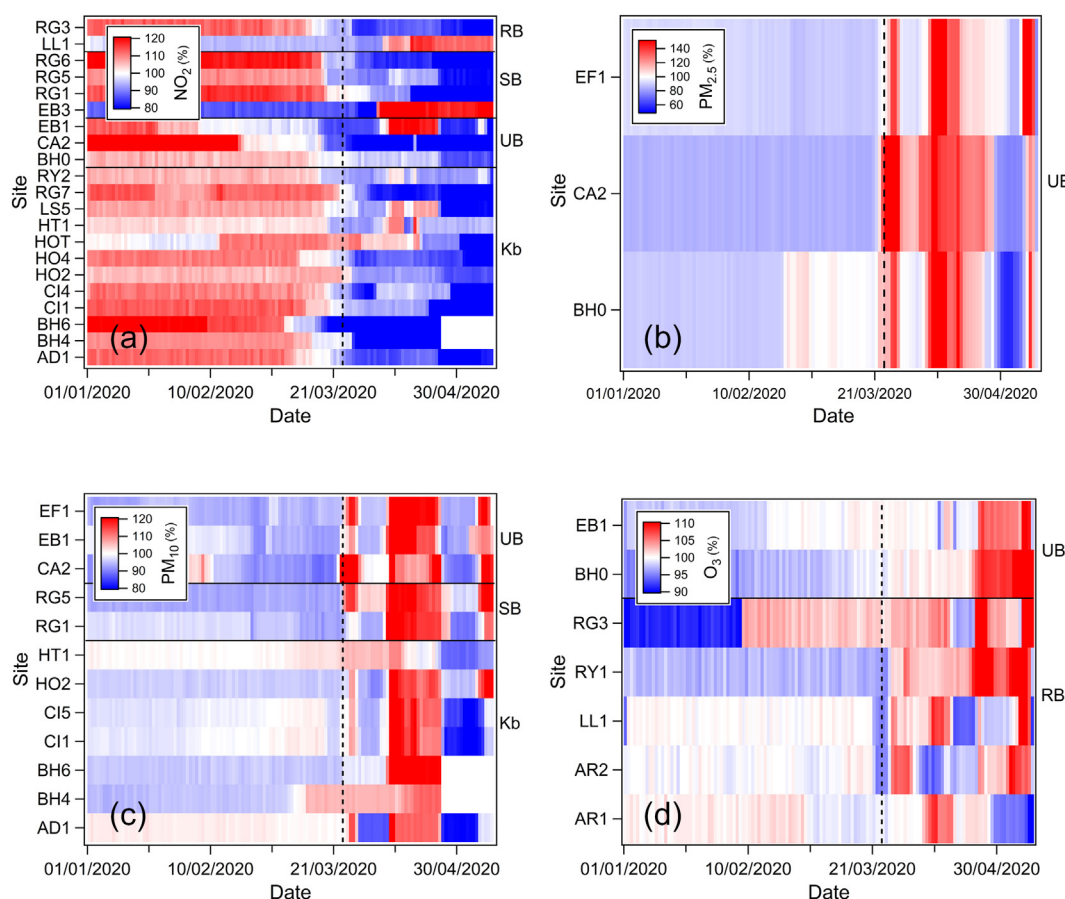


Fig. 1. Relative changes in 'de-weathered' air pollutant abundance in the southeast of the UK during the pandemic lockdown period (starting 24/03/2020; denoted by vertical dashed line) with respect to the 2020 average: (a) NO_2 , (b) $\text{PM}_{2.5}$, (c) PM_{10} , (d) O_3 . Data grouped by site; site identifiers: Kb = kerbside, UB = urban background, SB = suburban background, RB = rural background. See Table 1 for site codes.

and constrain the model were obtained from the suburban AURN facility in Eltham, south London. In order to reduce the complexity of the box model, it was constructed around oxidation mechanisms for the 27 NMHCs measured by Gas Chromatography coupled to Flame Ionisation Detection (GC-FID) in Eltham over the study period, these were: ethane, propane, n-butane, isobutane, isopentane, n-pentane, methyl-2-pentane, n-heptane, n-hexane, n-octane, ethene, propene, 1-butene, cis-2-butene, trans-2-butene, 1-pentene, trans-2-pentene, 1,3-butadiene, isoprene, ethyne, benzene, toluene, m- and p-xylene, o-xylene, ethylbenzene, 1,2,4-trimethylbenzene and 1,3,5-trimethylbenzene. Simulations were conducted for periods of 24 h, starting at midnight, and were constrained using appropriate hourly averaged measured data for NO_x , O_3 , NMHCs, CO, temperature and relative humidity and an average background level of $1275 \mu\text{g m}^{-3}$ methane. In total, the MCM subset employed comprised 2316 different species and over 7000 reactions.

3. Results

3.1. Changes observed by ambient monitoring networks

Fig. 1(a–d) shows the relative changes in the abundance of common ambient air pollutants NO_2 , $\text{PM}_{2.5}$, PM_{10} and O_3 with respect to the 2020 average (*i.e.* January–May, inclusive). A companion plot, showing the relative changes in air pollutant abundance relative to the 2015–2019 mean can be found in the Supplementary material (Fig. S3).

Fig. 1(a) shows that reductions in de-weathered NO_2 , relative to the 2020 mean, occurred at eighteen Sussex-Air and AURN monitoring stations which monitored NO_2 during the lockdown period. Significant

reductions can be seen at all kerbside sites, although with some variation. As shown in Table 2, NO_2 concentrations at kerbside sites were reduced to ~62% of the 2015–2019 average for March to May, inclusive. This represents an average 38% reduction in de-weathered NO_2 concentrations.

Fig. 2(a) shows the absolute changes in de-weathered NO_2 concentrations at kerbside monitoring stations in $\mu\text{g m}^{-3}$ since 1st January 2020. It shows that de-weathered concentrations at all sites in the network declined following the enforced lockdown period from 24th March 2020. However, there is a pattern of larger reductions adjacent to busier roads, likely reflecting the relative importance of road traffic emissions at these locations. For example, the greatest reductions were seen at RG7, CI1 and HOT (H05), of which RG7 and CI1 are located adjacent to the A23 and A27, respectively, which are major A-roads in the South East region of the UK.

During the lockdown period, de-weathered NO_2 concentrations fluctuated, with intermittent peaks evident in the time series data, however overall, de-weathered concentrations were generally below those of the preceding period (1st January to 23rd March 2020, inclusive) at all locations. In addition, the data in Table 2 show that the mean reduction across the study area was $10.7 \mu\text{g m}^{-3}$, relative to the 2015–2019 period mean for March to May, inclusive. For comparison, the equivalent mean reduction in NO_2 concentrations prior to de-weather analysis (*i.e.* simply the ambient values) was $11.7 \mu\text{g m}^{-3}$, which corresponds to a reduction of ~38% relative to the 2015–2019 period mean for March to May, inclusive.

Figs. 1(a) and 2(b) show the de-weathered NO_2 concentrations at background sites across the networks (urban, suburban and rural). Mean de-weathered concentrations declined at suburban background

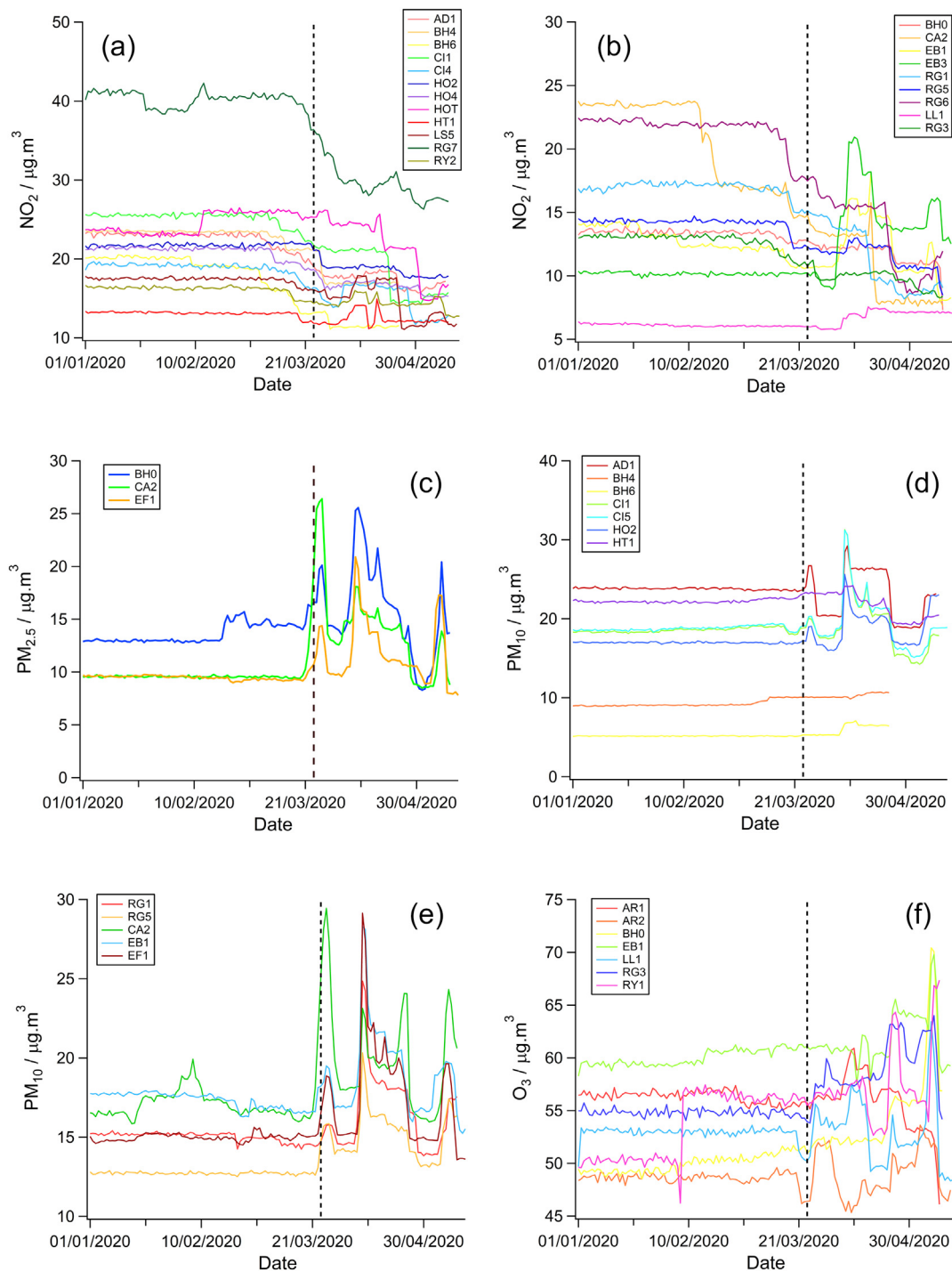


Fig. 2. Absolute changes in air pollutant abundance by monitoring site type in the southeast of the UK during the pandemic lockdown period (starting 24/03/2020); all data 'de-weathered' using concomitant meteorology parameters (see [Methodology](#)). (a) NO₂ kerbside, (b) NO₂ urban, suburban and rural background, (c) PM_{2.5} suburban and rural background, (d) PM₁₀ kerbside, (e) PM₁₀ urban and suburban background. (f) O₃ suburban and rural background. See [Table 1](#) for site codes.

sites (FAL, RG1, RG5 and RG6) to values ~63% of the 2015–2019 period mean for March to May, inclusive ([Table 2](#)). However, notably, de-weathered concentrations of NO₂ at EB1 and EB3 (urban background) and LL1 (rural background) (located on the south coast within ~7 km of each other) increased relative to the 2020 average, and the 2015–2019 baseline average for EB1 and EB3. For LL1, this is consistent with the findings of [Marner et al. \(2020\)](#), who showed that NO₂ concentrations at many rural sites across the UK were higher during the lockdown period. It should be noted that the temporal profile of the

increases in de-weathered NO₂ concentrations at EB1, EB3 and LL1 were well correlated, as shown in the time-series in [Fig. 2\(b\)](#). The increase is visible in the trendlines from approximately 28th March to 15th April 2020. The 7-day HYSPLIT back trajectory analysis in [Fig. 3](#) highlights that anticyclonic easterly mass air movements over North West Europe correlate with the increase in de-weathered NO₂ values at EB1, EB3 and LL1 and that air masses originating from the Atlantic and North Sea correlate with periods of background NO₂ values. Accordingly, despite the relatively short boundary layer lifetime of NO_x (*ca.*

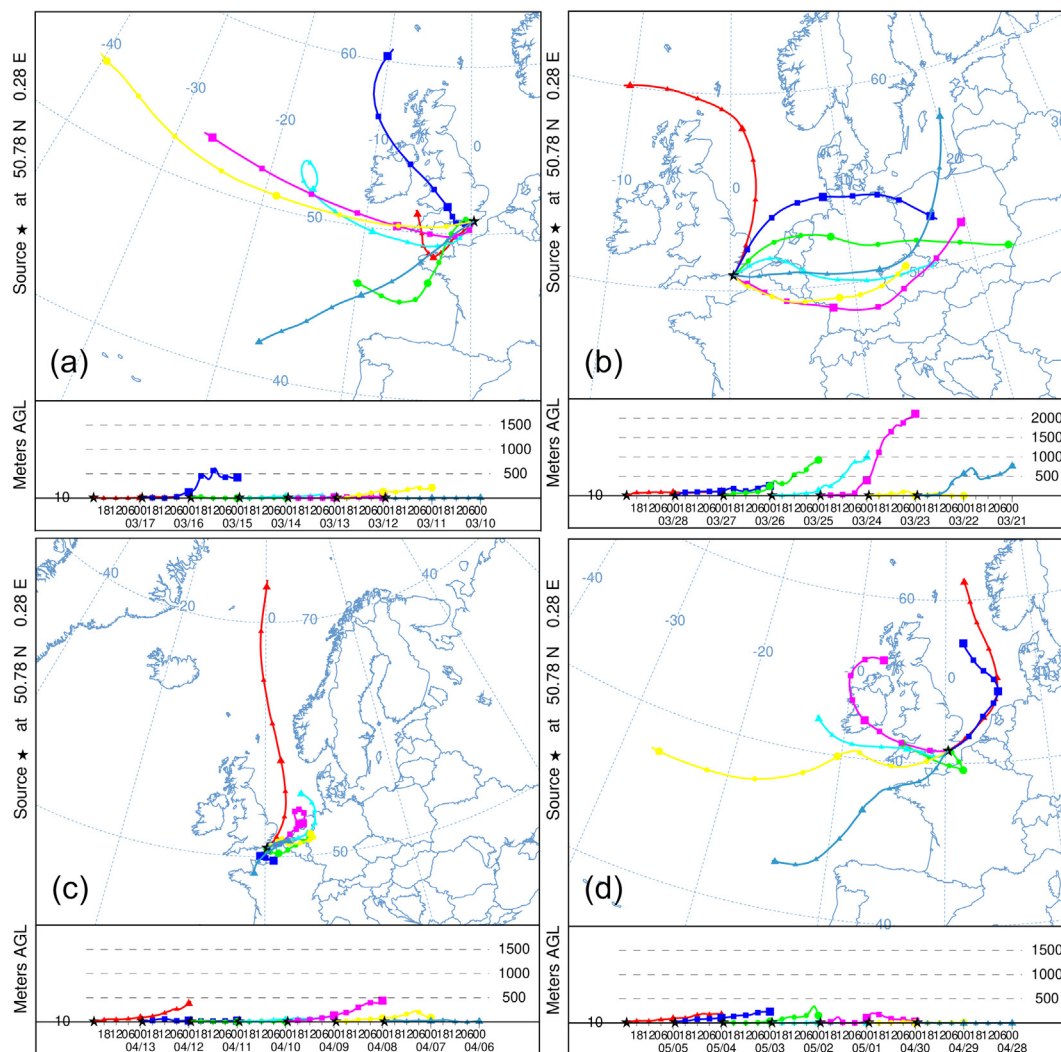


Fig. 3. 7-Day HYSPLIT back trajectory analyses for higher pollution periods identified in the southeast of the UK during periods (a) 10/03/2020–17/03/2020, (b) 21/03/2020–28/03/2020, (c) 06/04/2020–13/04/2020, and (d) 28/04/2020–05/05/2020. Model starting height = 10 m; time resolution = 6-h; starting location = Eastbourne (50.78 N, 0.28E).

hours – 1 day; e.g. Wenig et al., 2003; Liu et al., 2016), owing to the proximity of these particular receptor sites on the south coast of the UK to mainland Europe, it is possible that transboundary dispersion and transport of emissions from the heavily polluted regions of the North West of the continent (e.g. Hofman et al., 2016; Cordell et al., 2016; Wyche et al., 2020) had some degree of influence on the de-weathered NO_2 concentrations at these sites, despite a reduction in local emissions sources as a result of the UK lockdown.

Three monitoring stations, BH0, CA2 and EF1, monitor $\text{PM}_{2.5}$ concentrations at urban background locations in the AURN and Sussex-Air Network. There was a marginal increase in de-weathered $\text{PM}_{2.5}$ concentrations at these sites after the lockdown started, from 24th March 2020, relative to the 2020 mean, as shown in Fig. 1(b). In addition, de-weathered concentrations were ~106% of the 2015–2019 baseline mean for the same period, as shown in Table 2.

The time series of de-weathered $\text{PM}_{2.5}$ concentrations shown in Fig. 2(c) across all three monitoring stations were in good agreement. This is an important finding owing to the separation distance between the sites, which are located at Brighton Preston Park (BH0), Gatwick East (CA2) and Eastbourne Holly Place (EF1), and is indicative of regional, rather than isolated/local changes. There are three clearly defined peaks in the trendlines, first at the beginning of the lockdown period, secondly around the 8th April 2020, and again at the beginning of May 2020. These peaks correlate with regional pollution episodes

detailed above and again, can be explained from inspection of the HYSPLIT 7-day back trajectory analysis of mass air movements shown in Fig. 3. As discussed, during this period, anticyclonic easterly mass air movements caused transboundary transportation of pollutants such as NH_3 , O_3 , O_3 precursors and particulate matter (likely emanating from building emissions, fires, and industrial processes) from North West Europe to the UK, elevating local pollutant concentrations, as is a common occurrence in the South East region (AQEG, 2012).

Thirteen stations monitor PM_{10} concentrations in the AURN and Sussex-Air Network (eight at kerbside, three at urban background and two at suburban background locations). As shown in Fig. 1(c), relative to the 2020 average, de-weathered PM_{10} concentrations increased during the lockdown period, most notably during April. Fig. 2(e) and (f) show similar trends in de-weathered PM_{10} concentrations to those of $\text{PM}_{2.5}$, whereby there is good agreement in the data at all sites, and there are clearly defined peaks in de-weathered concentrations which correspond with the timing of regional pollution episodes, as shown in the back trajectory analysis in Fig. 3. As such, there is little evidence of an impact from traffic reductions owing to lockdown restrictions on ambient PM_{10} , as de-weathered concentrations were higher than the preceding months in 2020. However, both kerbside and background (urban and suburban) de-weathered concentrations of PM_{10} were ~86% of the 2015–2019 period mean for March to May inclusive, overall, as shown in Table 2. This equates to an average reduction of $3.1 \mu\text{g m}^{-3}$

across the network when compared to the same time period during the preceding 5 years.

Finally, there are nine monitoring stations within the networks employed which monitor ambient concentrations of O₃, one at kerbside, two in urban background, one in suburban background and five in rural background locations. As shown in Fig. 1(d), de-weathered daily O₃ concentrations increased at all of these sites, relative to the 2020 mean. Fig. 2(f) shows the equivalent timeseries plot of absolute de-weathered O₃ concentrations since 1st January 2020, which again illustrates the increase in ambient O₃ concentrations experienced during the lockdown period. In addition, the data in Table 2 show that de-weathered mean daily O₃ concentrations were on average ~105% of the 2015–2019 period mean for March to May, inclusive; this increase relative to the 2015–2019 mean for the same period equates to 2.9 µg m⁻³. The largest increases in de-weathered O₃ concentrations were observed in urban locations, where mean values increased in the range 5–15%. Of the five rural background locations investigated, two sites (LL1, AR2) showed a small decrease in de-weathered O₃ concentrations relative to the 2015–2019 mean. This decrease was only observed for AR2 in the ambient O₃ data before de-trend analysis, while LL1 exhibited a small increase in O₃ concentrations relative to the same period of the 5-year baseline, by ~4%. Looking further at the ambient O₃ data prior to de-trend analysis, it is noteworthy that the mean increase across the sites relative to the 2015–2019 baseline is somewhat larger than the de-weathered equivalent, being 4.9 µg m⁻³, i.e. an average increase across the region of ~8% (which breaks down to an average increase of 11% across urban locations and 5% across rural backgrounds).

Direct comparisons can be made between Fig. 2(b) and (f) where both NO₂ and O₃ concentrations are monitored at background sites LL1, BH0, RG3 and EB1. There is a negative correlation between NO₂ and O₃ at all of these locations. At BH0 and RG3, the coefficient of determination (R²) is 0.56 and 0.60, respectively, which suggests that NO₂ reductions had a moderate effect on O₃ increases at these sites. The R² value at LL1 and EB1 showed a very weak effect however, which could be due to increases in NO_x/NO₂ at these locations during the lockdown period.

The changes observed in O₃ concentrations likely result from perturbations to boundary layer NO_x-NHMC-O₃ chemistry (see Section 4), and to some extent to transport of O₃ and O₃ precursor species from mainland Europe. While it remains difficult, without complex chemical transport modelling, to separate the respective contributions of local factors and regional transport to local ambient O₃ levels (Monks et al., 2015), it is possible to infer the potential influence of regional O₃ and O₃ precursor species at the monitoring sites, by comparing the daily average concentrations of O₃ and PM_{2.5} (using the latter as a marker for transported pollution) with results from back trajectory modelling. In order to make this comparison, data were taken from the Brighton and Hove site (BH0; which monitors both PM_{2.5} and O₃), and the Lullington Heath (LL1; which monitors O₃) and Eastbourne (EF1; which monitors PM_{2.5}) sites, located within close proximity of one another (~7 km). To assist with analysis of the NO_x-NHMC-O₃ chemistry during the lockdown period, this comparison was also made for the suburban AURN site in Eltham (see Section 4).

Fig. S4 in the Supplementary material shows the daily average O₃ and PM_{2.5} data for BH0, LL1/EF1 and Eltham, alongside further results from HYSPLIT back trajectory modelling for key periods. As shown in Fig. S4 (and as discussed above), during periods of high PM_{2.5} concentrations at receptor sites, air masses originated from/passed over the air pollution 'hotspot' of North West Europe. As can also be seen in Fig. S4, there is some degree of correlation between O₃ and PM_{2.5} concentrations at these sites during certain time frames (e.g. 22/04/2020–25/04/2020), and occasionally with a time lag (e.g. 25/03/2020–30/03/2020). However, the overall correlation between daily PM_{2.5} and O₃ concentrations at the three sites over the period of 10/03/2020–05/05/2020 was relatively weak (i.e. R² for BH0 = 0.01, LL1/

EF1 = 0.11 and Eltham = 0.04). Collectively, this suggests that there was likely to have been some contribution to local O₃ concentrations in the South East from transportation of O₃ and O₃ precursors from mainland Europe, however, the time lags in the trendline, plus the presence of non-correlated peaks in O₃ (with respect to PM_{2.5}) suggest that increases in O₃ concentrations cannot solely be explained by inter-regional transport; see Section 4 for further details.

3.2. Changes observed by satellite remote sensing

Fig. 4 shows regional daily average NO₂ concentrations as recorded by TROPOMI over (a) the period 25/03/2019–22/04/2019 (i.e. the pre-pandemic baseline) and (b) 23/03/2020–20/04/2020 (i.e. post-implementation of lockdown restrictions). The percentage change between the two periods is also shown (c), as are the locally integrated values over the city of Brighton and Hove, plot alongside long-path DOAS measurements made on the ground (over a total path length 300 m) for the same time period (d).

The data shown in Fig. 4 confirms findings presented in Section 3.1 from analysis of the *in-situ* monitor observations made by the Sussex-Air Network and AURN, extending the reach of the data capture to the entire South East of the UK on a 7 × 7 km resolution scale. In-line with the *in-situ* monitors, TROPOMI measured a decrease in the concentrations of NO₂ across the entire region during the lockdown, with the regional average value falling by 33%, from 4.9 × 10¹⁶ to 3.3 × 10¹⁶ molec m⁻². Fig. 4(c) shows that the largest changes in NO₂ were observed in the centre of the region, in the areas surrounding London and at certain coastal locations.

As seen in Fig. 4(d), when integrated across the city scale (Brighton and Hove in this instance), TROPOMI is relatively successful in capturing local daily variations when compared to remote sensing conducted on the ground, in this case by long-path DOAS. Here, TROPOMI measured NO₂ values across the city during the 2020 lockdown period to be 59% of those measured over roughly the same time period the previous year (with mean values falling from 4.4 × 10¹⁶ to 2.9 × 10¹⁶ molecule m⁻²), comparing favourably with DOAS, which recorded NO₂ values that were ~64% of those measured during the previous two years over roughly the same time period (see Section 3.3).

3.3. Changes observed in high time resolution

Average diurnal profiles of pollutants measured by DOAS for March and April before (2018–2019) and after (2020) initiation of lockdown restrictions are shown in Fig. 5. As observed by the wider monitoring networks, ambient NO₂ throughout the average day was measured to decrease significantly during the lockdown period, by ~7 µg m⁻³, to values ~62% of those seen over the same time period during previous years. Although the average daily NO₂ value during the lockdown period was measured to be significantly lower, the typical bi-modal diurnal profile was maintained, with early morning (~05:00–09:00) and late afternoon/evening (~16:00–23:00) peaks in concentration. As is clear in Fig. 5, the morning peak, usually associated with commuter and transport activity (e.g. Melkonyan and Kuttler, 2012; Roberts-Semple et al., 2012; Hofman et al., 2016), did not reduce in magnitude after restrictions were imposed, although its duration did decrease by ~1 h; this is most likely indicative of the UK transport and delivery fleet maintaining operations on major UK road networks, such as the nearby A27, and citizens staying at home rather than commuting to their places of work. The high-time resolution NO₂ data shows therefore, that besides during the morning period (~05:00–07:00), anthropogenic activity responsible for NO_x emissions (primarily transport related in the UK; AQEG, 2004; DEFRA, 2020b), did decrease significantly throughout the day, by as much as ~13 µg m⁻³ later in the evening (~19:00), suggesting that citizens were conforming to mobility and distancing restrictions during hours typically associated with social activities. The peak in concentration during the morning period noted above,

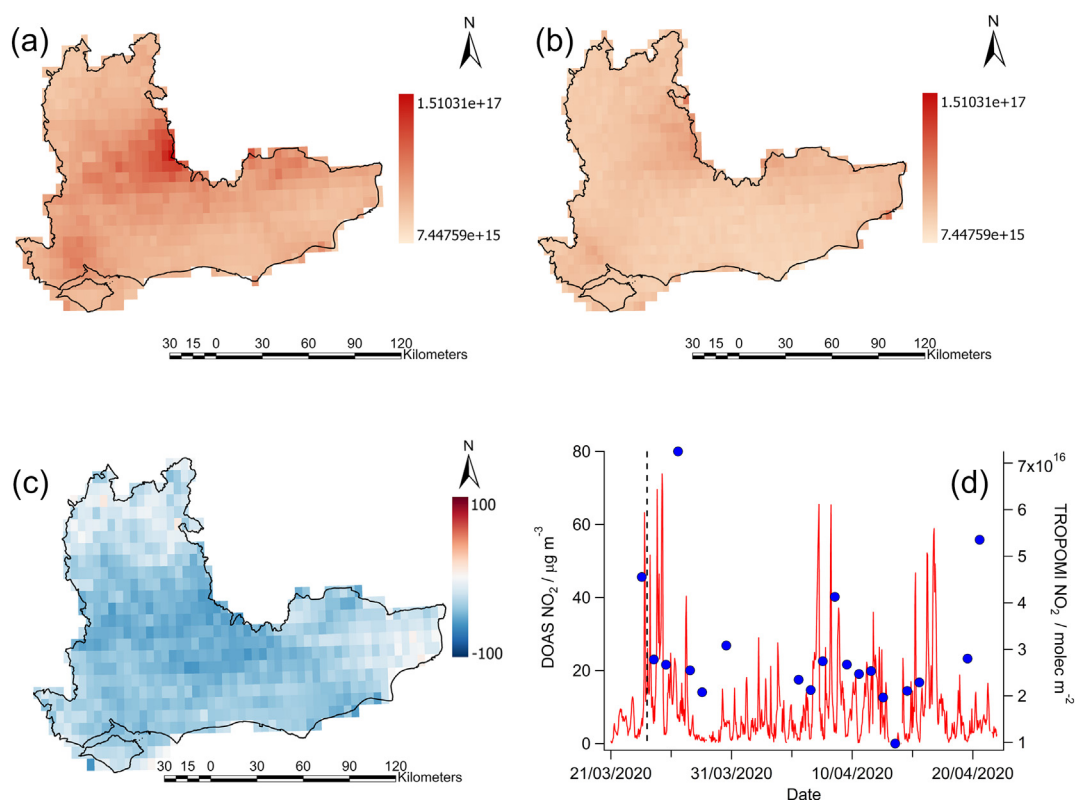


Fig. 4. (a) TROPOMI NO₂ data averaged over the South Eastern quadrant of the UK for the period 25/03/2019–22/04/2019 (*i.e.* baseline without restrictions) and (b) 23/03/2020–20/04/2020 (*i.e.* the start of the UK lockdown period). The percentage change between the two periods is also shown (c), along with area averaged NO₂ pixel values for Brighton (blue markers) compared to measurements made by DOAS (d). (For interpretation of the references to colour in this figure legend, the reader is referred to the web version of this article.) Data source: Copernicus Sentinel-5P Pre-Operations Data Hub.

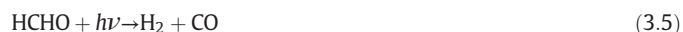
was likely influenced by Freight and Heavy Goods Vehicle movements, which continued during lockdown. Similar to ambient NO₂, concentrations of HONO were observed to decrease; with daily averages going down by almost 1 μg m⁻³ during lockdown to values ~74% of those seen over the same time period during previous years. With NO_x being a source of HONO (reactions (3.1)–(3.3); *e.g.* Harris et al., 1982; Aliche et al., 2002; Finlayson-Pitts et al., 2003), decreases in HONO are to be expected, in-line with falling (primary) vehicle emissions and ambient NO₂ values (Calvert et al., 1994; Harrison et al., 1996; Kirchstetter et al., 1996).



Comparable to other monitoring sites in the AURN and Sussex-Air Network, ambient daily O₃ concentrations measured by DOAS in the suburbs of Brighton and Hove were higher during the lockdown period, by an average of ~11 μg m⁻³, reaching values ~115% of those seen over the same time period during previous years, presenting with roughly the same diurnal profile (Fig. 5; *i.e.* with higher levels persisting slightly longer into the evening). As is well known, NO_x, O₃ and hydrocarbons exist in a complex photochemically induced balance within the troposphere (Monks, 2005), where depending on relative concentrations, a decrease in NO_x and an increase in solar radiation (as was observed during the lockdown period relative to previous years, see Fig. 5) can lead to an increase in the ambient O₃ concentration. O₃ production during the pandemic period is discussed in more detail in Section 4.

Average daily levels of formaldehyde (both a primary and secondary pollutant in sub/urban air; *e.g.* Parrish et al., 2012; Franco et al., 2016; Fu

et al., 2019) did not differ significantly during the lockdown period compared to previous years, *i.e.* the average daily formaldehyde concentration after lockdown increased by only ~0.2 μg m⁻³, to values 102% of those observed across the same time period during previous years. Interestingly, however, the formaldehyde diurnal profile did differ somewhat after the lockdown date. As can be seen in Fig. 5, hourly HCHO averages were higher between *ca.* 07:00 and 12:00 (by as much 20%) and lower between solar noon, *ca.* 13:00, and 18:00, presumably as photolysis (reactions (3.2) and (3.3)) and photochemical (reaction (3.4)) losses (Calvert et al., 1972; Fried et al., 1997; Pope et al., 2005; Parrish et al., 2012) were greater during the 2020 pandemic period when levels of solar radiation were significantly higher (by ~27% compared to the same period during 2019; Fig. 5).



Primary pollutants SO₂ and C₆H₆ were observed to increase in concentration during the average day after lockdown restrictions were imposed, with SO₂ increasing by 0.5 μg m⁻³ to values 125% those observed during previous years, and C₆H₆ increasing by ~1 μg m⁻³, to values ~147% of previous years. As is evident in Fig. 5, SO₂ and C₆H₆ diurnal profiles were largely similar before and after lockdown, with the exception of SO₂ between 19:00 and 23:00 h, where the evening peak was enhanced with restrictions in place, presumably owing to local activity. As noted in Section 2.2, C₆H₆ data reported here should be treated with caution and used as an indicative guide only, as measurements were typically on or below the DOAS sensitivity limit for this species during the measurement periods before and after lockdown. Absolute C₆H₆

values at the Falmer site in Brighton and Hove are likely to be significantly lower than those reported here.

4. Discussion

4.1. Boundary layer composition

It is now clear that changes in tropospheric trace composition occurred as a direct result of dramatically decreased anthropogenic activity during the anthropause of 2020, triggered by lockdowns imposed by governments in response to the COVID-19 global pandemic (e.g. Siciliano et al., 2020; Kerimray et al., 2020; AQEG, 2020a). As discussed in Section 3, data from across the AURN and Sussex-Air monitoring networks show that there was a clear overall decline in average ambient NO_2 across a range of environment types (urban – rural, kerbside – background) in the South East of the UK during the lockdown period, relative to the 2020 mean and the preceding 5-year baseline. It is now clear that these changes were principally owing to fewer vehicle movements during the UK during the lockdown period, by up to 70% by mid-April (AQEG, 2020a).

The impact of the lockdown on ambient PM concentrations is less clear. Overall, the data show a decrease in de-weathered PM_{10} concentrations across the environment range (by ~14%), and an increase in $\text{PM}_{2.5}$ (by ~6%), relative to the preceding 5-year mean. As was noted in

Section 3.1, there were clearly defined peaks in de-weathered PM_{10} and $\text{PM}_{2.5}$ concentrations across the South East of the UK during the lockdown period, which corresponded with regional pollution episodes, where interregional transport brought the continental plume across to the UK. As a result, there is limited evidence of a decline in particulate matter concentrations during the UK lockdown which can be attributed directly to reductions in local traffic volumes in the South East. Accordingly, more research is needed to understand the impact of lockdown measures on PM chemical composition and the abundance of PM precursors (AQEG, 2020a) in order to investigate any potential shifts in PM abundance and size distribution, such as increases in concentrations of UFPs. Such an investigation would require complex coupled emissions, physio-chemical and transport modelling, and is beyond the scope of this work.

The data also show that with the decrease in NO_2 , there was a concomitant increase in average ambient daily O_3 concentrations at kerbside, urban background, suburban background and rural background sites, relative to both the 2020 mean and the preceding 2015–2015 baseline, with the biggest increases observed under urban conditions. This trend is consistent with the findings of other authors and is not limited to the UK (e.g. Siciliano et al., 2020; Kerimray et al., 2020; AQEG, 2020a).

As shown in Fig. 2(f), absolute de-weathered concentrations of O_3 at urban sites were largely comparable to several rural locations during

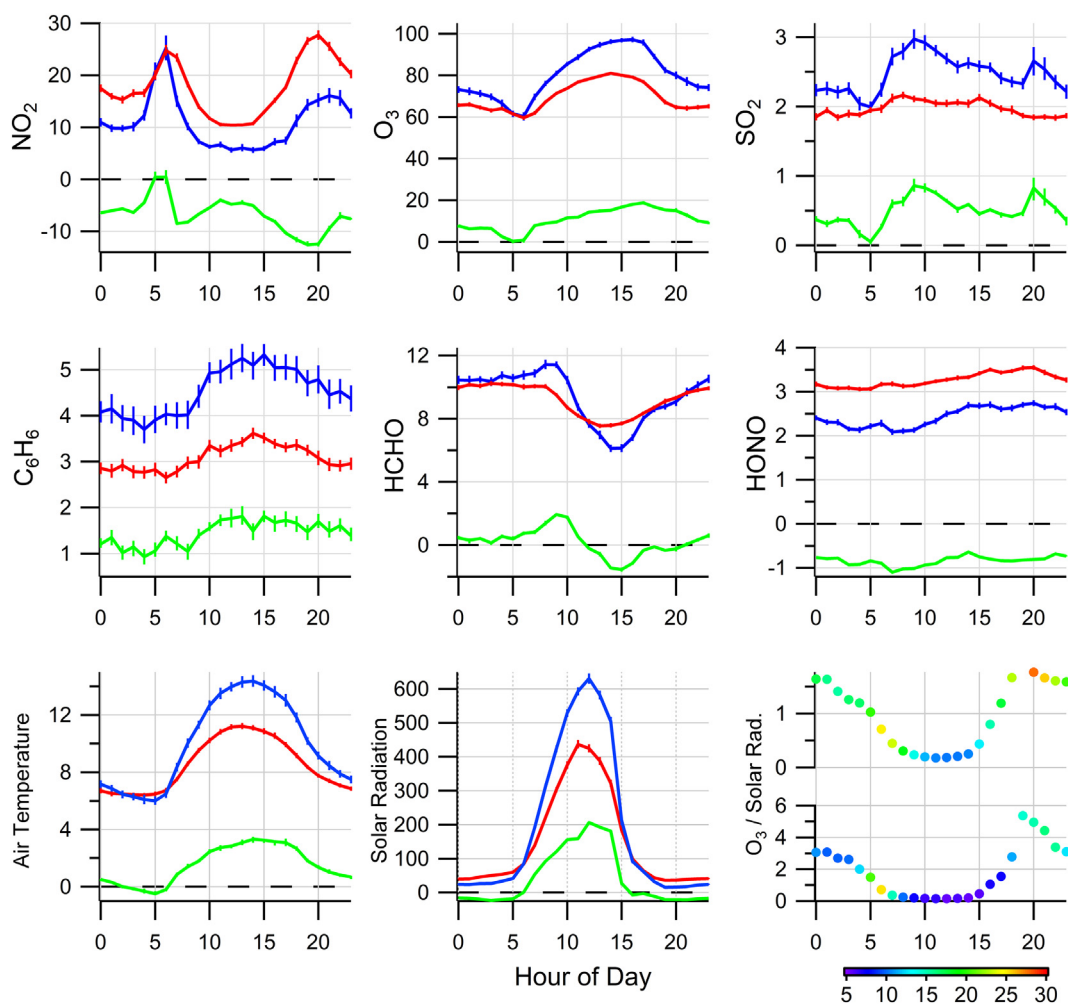
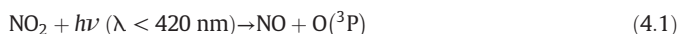


Fig. 5. Average diurnal evolution of trace gases measured by DOAS ($\mu\text{g m}^{-3}$), temperature ($^{\circ}\text{C}$) and solar radiation (Wm^{-2}) during the pandemic lockdown period (starting 24/03/2020; blue line), compared to their average diurnal pattern for the same time period during the preceding 2-years (i.e. March and April 2018–2019, inclusive; red line). The difference between the two datasets (i.e. the 2020 lockdown period and the March and April 2018–2019 baseline) is also shown (green line), along with the O_3 /solar radiation ratio (bottom right), coloured by NO_2 concentration ($\mu\text{g m}^{-3}$). (For interpretation of the references to colour in this figure legend, the reader is referred to the web version of this article.)

the lockdown period. Indeed, this urban rise toward concentrations typical of rural sites is expected owing to the reduction in titration of O₃ by nitric oxide (NO) as NO_x emissions reduced (e.g. Monks, 2005).

Owing to a larger production footprint and interregional transport at certain times during lockdown, there was likely some contribution to local O₃ levels in the South East of the UK from the transport of O₃ and O₃ precursors from polluted regions of North West Europe (Monks et al., 2015; AQEG, 2009). However, as shown in Fig. S4, the time lag between the O₃ and PM_{2.5} trendlines and the presence of isolated peaks in O₃, suggest there were significant contributions to local O₃ concentrations derived from changes in UK emissions. Importantly, these findings are not limited to the UK, with other studies from a range of countries also showing that tropospheric O₃ concentrations increased owing to changes in emissions profiles during lockdown, including in Spain (Tobías et al., 2020), Brazil (Siciliano et al., 2020), Italy, (Sicard et al., 2020), China (Chen et al., 2020; Le et al., 2020; Zhang et al., 2020), Korea (Ju et al., 2020) and India (Sharma et al., 2020).

If the $\Sigma(\text{NO}_2 + \text{O}_3)$, *i.e.* 'O_x', is observed over the 2020 period, it becomes clear that the overall abundance of total O_x species did not change significantly as a result of the UK lockdown, as can be seen for example in Fig. 6, which shows daily mean NO₂ and O₃ concentrations measured by DOAS during 2020 in Brighton and Hove. The anti-correlation observed between NO₂ and O₃, as NO_x emissions reduced during the COVID-19 anthropause, can also be seen in higher time resolution during the typical diurnal cycle, as shown in Fig. 5. The preservation of total O_x species witnessed here is the result of well known tropospheric NO_x-O₃ photochemistry in polluted air (Monks, 2005), principally:



where M is a reaction third body. Fig. 5 clearly shows that over the average diurnal cycle in the spring of 2020, more solar radiation (hence actinic flux) was available at ground level to initiate tropospheric photochemistry (e.g. Madronich, 1993; Kleinman, 1994; Monks, 2005). As seen from the O₃:Solar Radiation (O₃:SR) ratio (Fig. 5, bottom right), the increase in both solar radiation and O₃ were well correlated, with O₃:SR ratios being roughly the same throughout daylight hours (*i.e.* ca. 07:00–17:00) during the lockdown period as during the baseline year (*i.e.* 2019 in this instance for local meteorology data in Brighton and Hove). The major differences noted in O₃:SR ratios between 2020 and 2019 occurred during the early morning and late afternoon, *i.e.* periods marked by higher ambient NO₂ concentrations. Further to this, it is clear from Fig. 5 that during the UK lockdown period, where NO_x emissions were reduced, O₃ persisted longer, at higher

relative concentrations, during nocturnal hours, owing to lower ambient concentrations of NO, and a decrease in O₃ scavenging *via*:



However, NO_x-O₃ photochemistry is highly non-linear and also involves the oxidation of hydrocarbons and the production and cycling of hydro (HO₂) and organic (RO₂) peroxy radical species (e.g. Haagen-Smit and Fox, 1954; Sillman, 1999; Salisbury et al., 2002; Monks, 2005). Thus, to fully understand the changes observed in tropospheric composition (and reactivity) during the UK lockdown period, hydrocarbon and radical species must also be considered.

It should be noted that at certain stations, where NO₂ spikes were noted, e.g. at Eastbourne/Lullington Heath (see Figs. 1 and 2), total O_x levels increased transiently during the aforementioned transboundary pollution episodes (e.g. 09/04/20 and 24/04/20) owing to transported pollution from mainland Europe (see Figs. 3 and S4). This is most likely a result of short-lived, continental NO_x persisting long enough to influence local O_x concentrations in the UK during transport and before titration from the boundary layer (*i.e.* typical NO₂ lifetime in interregional plumes is <1 day).

As discussed in Section 2.4, there were no comprehensive NMHC monitoring sites available in the Sussex-Air Network or AURN in the South East of the UK from which to acquire hydrocarbon data for this study. As such, data were acquired from the nearest available facility, *i.e.* the suburban AURN site in Eltham, south London. Changes in the NO₂ and O₃ data obtained from Eltham were largely consistent with those observed across the South East UK AURN and Sussex-Air Network, and thus the site offers a valid reference point for this study. More specifically, at Eltham, average ambient 2020 NO₂ values were down by ~6 μg m⁻³, to values ~65% of those seen over the same time period over the baseline years of 2015–2019 (c.f. non-de-weathered data from the suburban FAL site in Brighton and Hove: ~7 μg m⁻³ and 64%), total NO_x values were down by ~8 μg m⁻³, to values ~66% of the baseline, and 2020 O₃ values were up by ~11 μg m⁻³, to values ~122% of those seen previously over baseline years (c.f. non-de-weathered data from the suburban FAL site: ~8.4 μg m⁻³ and 112%).

From the Eltham GC-FID measurements, it was determined that over the spring of 2020, during the UK lockdown period, total ambient NMHC concentrations were ~3 μg m⁻³ lower than the average of the same period between 2015 and 2019, *i.e.* 2020 total NMHC concentrations had reduced to values ~83% of those typically expected over the spring months. Of the hydrocarbon fractions, aromatics were found to have proportionally decreased the most, *i.e.* to levels ~66% of previous years (an absolute change of ~-0.7 μg m⁻³), followed by alkanes (~84%, ~-2 μg m⁻³) and then alkenes (~94%, ~-0.1 μg m⁻³). This finding is somewhat expected, with road transport comprising a major source of aromatic hydrocarbons (e.g. Brocco et al., 1997; Kerbachi et al., 2006;

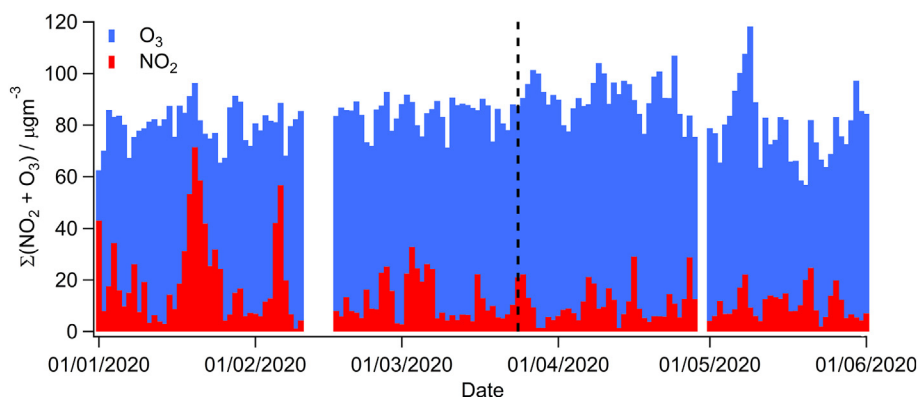


Fig. 6. Total daily O_x (*i.e.* NO₂ + O₃) measured by DOAS at the suburban Falmer site, using stacked daily averages. Black dashed line indicates the start of the UK lockdown period (24/03/2020).

Correa and Arbilla, 2006) and road transport activities having reduced significantly during the UK lockdown (total motor vehicle use dropping to a low of 23% of typical values on 13/04/2020; DfT, 2020).

The NO_x -NMHC- O_3 relationship is best visualised using a surface plot, where NO_x and NMHC are plotted with their corresponding O_3 contours, or 'isopleths' (Sillman, 1999); such a plot for the atmosphere of Eltham is shown in Fig. 7(a), constructed using monthly averaged measurements between 1st January 2015 and 1st June 2020.

Fig. 7(a) shows a regime where the boundary layer air over Eltham is generally characterised by a total NO_x load that is greater than the total (measured) NMHC load, and where higher O_3 concentrations typically result from lower absolute values of both species. Fig. 7(b) shows the same data presented as a scatter plot of O_3 vs. NMHC: NO_x ratio, which presents a roughly increasing O_3 concentration profile with NMHC: NO_x ratio, as is typically seen under urban conditions (e.g. Finlayson-Pitts and Pitts, 1993; Wolff and Korsog, 1992; Monks, 2005; Tobías et al., 2020). Both plots also show the relative positions of atmospheres in the NO_x -NMHC- O_3 space before (labelled: 'Baseline Years') and during the lockdown period (labelled: 'Pandemic Year'), using data averaged appropriately over March, April and May for 2015–2019 and 2020, respectively.

The Eltham springtime boundary layer (for the baseline years and the pandemic year) sits within a NMHC (sensitive) limited regime (Sillman, 1999), as is common with many urban atmospheres (e.g. Finlayson-Pitts and Pitts, 1993; Monks, 2005), where an increase in ambient NMHCs (at constant NO_x concentration) would cause an increase in O_3 concentration, and where an increase in ambient NO_x (at constant NMHC concentration) would cause a decrease in O_3 concentrations, and vice versa. As shown in Fig. 7(a) and (b), a greater decrease in concentrations of ambient NO_x species occurred during the UK lockdown period, relative to the 2015–2019 baseline, than total ambient NMHCs, i.e. the former seasonal (i.e. March, April, May) average decreasing by 33% and the latter only by 17%, such that the NMHC: NO_x ratio increased from 0.70 to 0.87. In a NMHC limited regime under sufficient actinic flux, this led to an increase in ambient O_3 concentrations during lockdown, which is clearly shown in Fig. 7(a) and (b), with the atmosphere transitioning to a higher O_3 concentration isopleth and higher O_3 concentration point, respectively. This change in atmospheric composition is most likely rooted in the non-linear reductions that occurred during lockdown, in emissions of pollutant trace gases across a ranges of

sources, with road traffic (the principle source of UK NO_x emissions; NAEI, 2019a, 2019b) reducing significantly after restrictions were imposed, as many citizens remained in their homes, while other 'key' industries (which are known to emit NMHCs) continued to operate (AQEG, 2020b). To illustrate, National Atmospheric Emissions Inventory data (NAEI, 2019b) shows that the largest sources of NMVOC (NMHC) emissions in the UK are industrial processes and product use (53% of the UK total), extraction of fossil fuels (19%) and agriculture (13%).

As noted in Section 3.1, mean de-weathered O_3 concentrations were found to have increased a greater amount across the various urban environments than in rural backgrounds (i.e. 10% vs. 1%), and that mean de-weathered O_3 values had decreased slightly relative to the 5-year baseline at rural background sites LL1 and AR2 (Table 2). With no NMHC data available at the AURN and Sussex-Air sites in the South East of the UK, it is not possible to conclusively comment on potential underlying chemistry at these locations, however as noted above, it is common for urban locations to reside within the NMHC limited regime and for rural background environments to reside within the NO_x limited regime. Despite observed potential influences from interregional transport, the mean de-weathered NO_2 concentrations across the three urban location types was ~33% lower during the lockdown period than over the 2015–2019 baseline, and across rural background sites, was ~22% lower. Such a decrease in ambient NO_2 within the NMHC limited O_3 production regime of urban locations will have resulted in an increase in net O_3 production, whereas reducing NO_x under rural, NO_x sensitive conditions, is likely to have resulted in a decrease in net O_3 production (presuming in both cases a roughly constant NMHC loading) (Finlayson-Pitts and Pitts, 1993; Sillman, 1999; Monks, 2005).

4.2. Boundary layer reactivity

As is well known, the OH radical and the O_3 molecule are the primary oxidants of the sunlit troposphere, and their abundance will control tropospheric 'oxidative capacity', i.e. "the diurnal mean ability of the [troposphere] to oxidise trace compounds" (Monks, 2005). In essence, the abundance of OH and O_3 will control how 'reactive' the troposphere is.

O_3 photolysis in the presence of water vapour is the primary daytime source of the tropospheric OH radical (Levy, 1971):

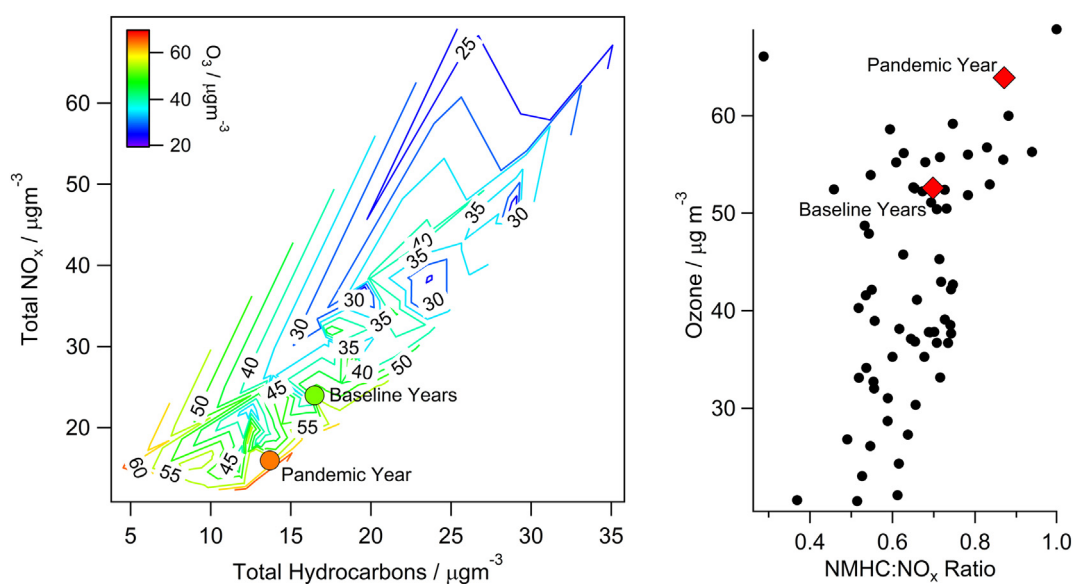
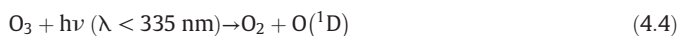


Fig. 7. Ozone isopleth plot for the AURN suburban Eltham site in outer London (a) and corresponding ozone versus hydrocarbon: NO_x ratio relationship (b) using monthly averaged data between 01/01/2015 and 01/06/2020. The respective atmospheric positions for averages taken over March, April and May over the 'baseline years' (2015–2019) and for the corresponding average taken during the 'pandemic year' (2020) are shown.



It follows then, that a suitably humid, daylight troposphere with increased O_3 loading would generate more OH and (depending on loss routes) have a higher overall oxidative capacity, or 'reactivity' (Lelieveld and Dentener, 2000; Monks, 2005; Yang et al., 2016), and be characterised by a greater production rate of secondary trace species (e.g. Atkinson, 2000; Calvert et al., 2002; Calvert et al., 2008).

In order to investigate the change in radical species, and hence atmospheric oxidative capacity/reactivity experienced during the lockdown period, a 0-D box model was constructed using inorganic and organic oxidation mechanisms extracted from the Master Chemical Mechanism website (<http://mcm.leeds.ac.uk/MCM/>). In order to create an approximation of local boundary layer air for the average springtime diurnal cycle before and after lockdown, models were run constrained with average measured NO_x , O_3 , NMHC, CO, CH_4 , temperature and relative humidity data (see Section 2.4 for details); the results are given in Fig. 8.

Fig. 8 shows the diurnal profile data for NO_x , O_3 and the sum of NMHCs before and during lockdown, as employed to constrain the 0-D box model. Fig. 8 also shows simulated end-stage organic reaction products, formaldehyde (HCHO) and methyl glyoxal (MeGly), which derive from the atmospheric oxidation of a range of organic primary pollutants (e.g. Atkinson, 2000; Calvert et al., 2002; Calvert et al., 2008 and references therein). Despite the 2020 model being constrained to a daily average NMHC loading 17% lower than the 2015–2019 baseline simulation, the daily average modelled secondary formaldehyde and methyl glyoxal values were 87% and 117% higher, respectively, in lockdown air compared to their respective baselines, indicating a more reactive atmosphere during 2020. The modelled concentrations of such secondary species represent an estimate in this instance; as shown in the measured data obtained from the DOAS system in Brighton and Hove (Fig. 5), HCHO values were higher before midday and lower around, and after, solar noon during lockdown. This is likely due to a combined result of a different NMHC loading in the local atmosphere of Brighton, and the higher levels of solar radiation experienced in the UK during the 2020 lockdown period, hence increased branching toward photolytic destruction of such photolabile species as HCHO (e.g. Calvert et al., 1972; Fried et al., 1997; Pope et al., 2005), which is not directly accounted for in the MCM model employed here.

The results obtained from the 0-D box model also indicate that after the 2020 lockdown was imposed, OH, HO_2 and RO_2 radical levels were significantly higher than average modelled values calculated over the same time period during baseline years, by 109, 245 and 259%, respectively. As well as an increased radical loading, the MCM model also suggests that there was a shift in partitioning between atmospheric HO_x / RO_x species after government restrictions were imposed, where both OH: HO_2 and OH: RO_2 2020 ratios were lower than the 2015–2019 baseline. This is indicative of an increase in forward cycling of OH to HO_2 and RO_2 via reaction with CO and organic species (RH), and a concomitant decrease in recycling of HO_2 and RO_2 back to OH via reaction with (reduced) NO (Monks, 2005), via:



Fig. 8 also gives the daily modelled temporal profiles of reservoir species, hydrogen peroxide (H_2O_2) and nitrous acid (HNO_3), before

and after lockdown. Owing to their propensity to partition out of the gas phase, both H_2O_2 and HNO_3 are able to terminate the chain cycling of tropospheric radical species (Lee et al., 2000):



As expected in a NMHC sensitive regime, formation of HNO_3 comprises the dominant chain termination route and radical sink (Monks, 2005), with modelled H_2O_2 : HNO_3 ratios of ~0.01 in both cases.

It is clear from Fig. 8 that the modelled concentrations of both H_2O_2 and HNO_3 were slightly larger in 2020, with their daily averages being ~112% of their 2015–2019 baseline values. By comparing the modelled radical recycling to chain termination routes and the modelled HO_x : NO_x ratios, the simulation suggests that during the lockdown period, branching shifted toward more radical chain cycling/propagation and away from termination via loss routes, with the daily average modelled HO_2 : H_2O_2 , RO_2 : HNO_3 and OH: HNO_3 ratios being larger within the 2020 simulation than that of the 2015–2019 baseline, and the OH: NO_x , HO_2 : NO_x and HO_x : NO_x ratios all increasing by roughly a factor of five in the 2020 simulation. Collectively these results suggest that the dominance of radical cycling over termination routes increased after government restrictions were imposed.

In addition, with reduced ambient HONO concentrations (see Section 3.3), and HONO being widely recognised as an important radical source in the early part of the day in the sub/urban atmosphere (e.g. Harris et al., 1982; Calvert et al., 1994; Harrison et al., 1996; Finlayson-Pitts et al., 2003), it is likely that the daily temporal profile of atmospheric reactivity would also have changed during lockdown, as would the overall contribution of typical OH sources to the OH budget. The combined measured and modelled data presented here point toward a relative decrease in OH production (and hence tropospheric reactivity) during early hours of the day, and a relative increase in OH production (and hence tropospheric reactivity) around and after solar noon. Such a perturbation to the reactivity profile of the boundary layer would clearly have a knock-on effect on a range of atmospheric phenomena in both the gas- and particle-phases.

Here, the MCM model simulations comprise only an aid to interpret measured data and a guide to relative changes in atmospheric composition (and hence oxidative capacity/reactivity), which resulted from the rapid changes in air pollutant emissions during the spring of 2020 after lockdown restrictions came into force. Simplifications made in the construction of MCM oxidation schemes have been discussed in detail elsewhere (Jenkin et al., 1997; Saunders et al., 2003), but in brief, include (i) exclusion of routes to "low-probability reaction channels"; (ii) abridged oxidation schemes for "minor" species and those not well characterised; and (iii) peroxy radical parameterisation to reduce complexity.

4.3. Future implications

The COVID-19 pandemic has provided a unique opportunity to test the atmospheric response to rapid, widespread anthropogenic emissions reductions. It has enabled the 'real-world' simulation of the potential impact of policy interventions to reduce certain pollutant emissions in the long-term and move society toward a low carbon future (Monks, 2020).

It is clear that significant NO_x reductions have resulted from governments around the world imposing lockdown restrictions on everyday life (e.g. Sicard et al., 2020). However, as presented here, owing to the complex, non-linear nature of tropospheric chemistry, mass reductions in individual pollutants can cause an increase in others, and can trigger changes in wider tropospheric trace composition and reactivity. In this study, the data show that total O_x species were preserved during the UK lockdown, with an increase in tropospheric O_3 concentrations

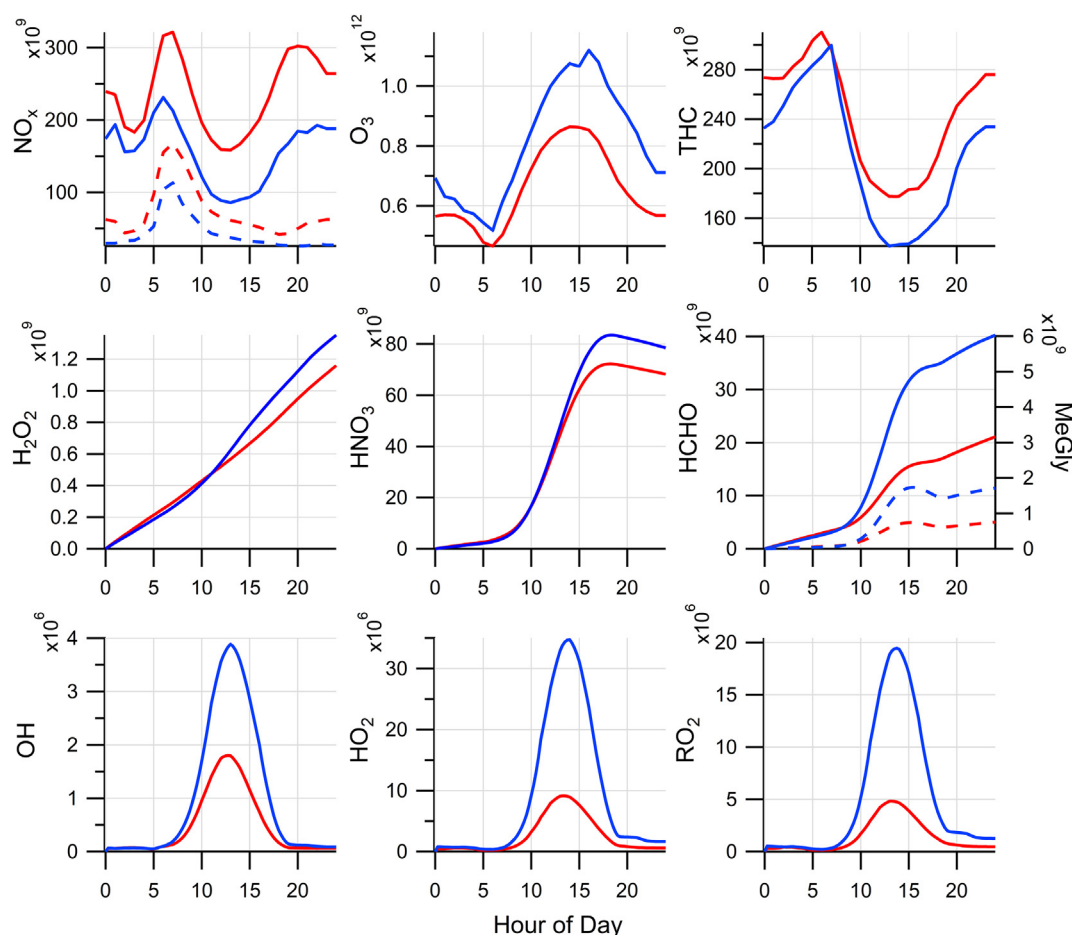


Fig. 8. Average diurnal evolution of trace gases (NO , NO_2 , O_3 and the 15 most abundant NHMCs; molecules cm^{-3}), temperature (K) and relative humidity (%), with modelled formaldehyde (HCHO; molecules cm^{-3}) and methyl glyoxal (MeGly; molecules cm^{-3}) and radical species (OH , HO_2 and RO_2 ; molecules cm^{-3}) during the pandemic lockdown period (starting 24/03/2020; blue line), compared to their average diurnal pattern for the same time period during the preceding 5-years (*i.e.* March and April 2018–2019, inclusive; red line). Measurement site: Eltham, south London. Note: in the NO_x panel, NO_2 is given by solid lines and NO by dashed lines; also, in the HCHO/MeGly panel, HCHO is given by solid lines and MeGly by dashed lines. (For interpretation of the references to colour in this figure legend, the reader is referred to the web version of this article.)

under the NMHC limited O_3 production regime (where total NO_x decreased proportionally greater than total NMHCs), and an increase in overall boundary layer reactivity.

The adverse health effects of acute and chronic exposure to both O_3 and NO_2 are well documented, with links to significantly exacerbated cardiovascular morbidity, diabetes, airway oxidative stress and asthma (*e.g.* Zhang et al., 2019; Travaglio et al., 2020). While there is limited recent comparative evidence which explores the health effects of the two pollutants in isolation, owing to their synergy in atmospheric composition, there is evidence that O_3 exposure can cause greater lung damage than NO_2 at the same concentration, and that NO_2 concentrations up to 20 times higher than O_3 could lead to comparable health effects; such findings suggest that O_3 is a more harmful pollutant to human health (*e.g.* Crapo et al., 1984; Mustafa et al., 1984). As such, we urge caution in the statement that there were comprehensive improvements in air quality as a result of the UK lockdown during the COVID-19 pandemic, owing to potential health effects from exposure to increased concentrations of O_3 , particularly in urban environments. Indeed, AQEG (2009) have previously predicted that long-term reductions of NHMC and NO_x emissions, by 60% or more, would be necessary to reduce O_3 concentrations in urban areas throughout the UK and Europe, owing to increases which result from the decreased suppression of O_3 by NO . As noted by Zhang et al. (2019), substantial reductions in fossil fuel consumption are needed to reduce NO_x and NHMCs (VOCs), as well as greenhouse gas emissions, in order to reduce the impact of O_3 on human health.

There is also an emerging body of evidence which seeks to link long-term exposure to poor air quality with susceptibility to, and severity of, COVID-19 symptoms. Alipio (2020) found that the number of cases of the virus was positively related to higher O_3 concentrations based on analyses from 34 different countries, while Travaglio et al. (2020) found that O_3 concentrations were significantly associated with COVID-19-related deaths, together with population density.

Studies have also started to look at linkages between COVID-19 and exposure to particulate matter (*e.g.* Cole et al., 2020; Wu et al., 2020), where Cole et al. investigated this linkage in the Netherlands, while Wu et al. investigated the linkage in the United States. In both studies, an increase in $\text{PM}_{2.5}$ concentrations by just $1 \mu\text{g m}^{-3}$ was positively associated with an increase in COVID-19 cases. There is also emerging evidence of a role for particulate matter in the airborne transmission of COVID-19, in particular PM_{10} , with some early results indicating that the virus could be present on PM in ambient air (*e.g.* Setti et al., 2020; Tung et al., 2020; Comunian et al., 2020; Manoj et al., 2020). With further research needed to support these early studies, the issue of PM air pollution is likely to be central to future discourse surrounding respiratory diseases.

While recent action at the policy level has been focused on reducing the adverse health effects of human exposure to NO_2 (DEFRA, 2017) and particulate matter, impacts of the lockdown (as presented herein) highlight that targeted emissions reductions must be applied across the species range. As shown from evidence in the United States and in China (Zhang et al., 2019), non-compliance with health-based O_3 standards

has been attributed to regulatory regimes seeking only to reduce anthropogenic emissions of NO_x and PM, while NMHC/VOC emissions remained constant (Finlayson-Pitts and Pitts, 1993; Pun et al., 2003). Furthermore, Le et al. (2020) argue that regulatory protocols aimed at reducing NO_x from road traffic serve only to limit progress in reducing concentrations of PM and O₃, where simultaneous regulatory controls to reduce emissions from power plants and industrial processes are not also implemented. Accordingly, it is vital that future policies to control and reduce emissions and ambient concentrations of air pollutants fully consider the complex trace composition and reactivity of the atmosphere, and that such findings as discussed herein should guide the implementation of strategies based on intelligent reduction mechanisms which consider a range of pollutant species and environmental conditions.

In order to ensure both health and air quality policy is effectively informed, there is now a pressing need for further studies (including simulation chamber experiments and model development and implementation) across a range of scenarios (e.g. NHMC/NO_x regimes and emission spectra) and long-term, detailed atmospheric measurements of baseline and event conditions.

5. Conclusion

The COVID-19 pandemic led governments around the globe to place restrictions on anthropogenic activity to halt the spread of the disease. Such restrictions caused a rapid decline in primary emissions, and in turn, a decline in ambient concentrations of certain air pollutants, most notably reductions in NO_x from road traffic sources. Such reductions over a relatively short time interval is entirely unprecedented and has provided the research community with an opportunity to investigate the atmospheric response to potential policy interventions which seek to reduce pollutant emissions in the long-term.

In this work, we have combined air quality monitoring data from the UK's AURN and Sussex-Air monitoring network with data from the University of Brighton JOAQUIN Advanced Air Quality reSearch laboratory and ESA's Sentinel-5P satellite, and findings from detailed chemical modelling, to investigate changes in tropospheric composition and reactivity in the South East of the UK during the 2020 COVID-19 pandemic.

The results presented have shown that there was a clear decline in average ambient NO₂ during the UK lockdown period, effective from 24th March 2020, owing to a reduction in vehicle traffic by as much as 70%. However, there was also a concomitant increase in average ambient O₃ concentrations (most noticeably under urban, hydrocarbon limited ozone production conditions), and the overall abundance of total O_x species did not change significantly at chosen study locations as a result of the UK lockdown. Our model simulations indicate that in environments that experienced a significant increase in O₃ loading during lockdown, the average daily abundance of OH would also have significantly increased (by 109% for the Eltham example investigated here). Combined with higher ambient O₃ concentrations, this would have led to an increase in boundary layer oxidative capacity/reactivity. As such the scenario is somewhat complex, and attention must also be given to the wider altered trace composition and reactivity of the atmosphere that occurred during lockdown, as well as the significant reductions in emissions of NO_x species, as have widely been publicised.

It has also been shown that there were clearly defined peaks in PM₁₀ and PM_{2.5} concentrations with respect to the 2020 average, which corresponded with the timing of regional pollution episodes. As a result, there is limited evidence of a decline in particulate matter concentrations which can be attributed to lockdown restrictions. As such, more research is needed to investigate potential shifts in particle size distribution, PM chemical composition and the abundance of PM precursors as a result of a decline in anthropogenic activity, which have the potential to lead to increasing concentrations of UFP fractions.

It is vital that future policies to control and reduce emissions fully consider the complex trace composition and reactivity of the

atmosphere. As pandemics are predicted to become more regular, there is now both a global need for pollutant emissions reductions to combat poor air quality and climate change, and for a better understanding of atmospheric effects and interactions with such diseases.

CRedit authorship contribution statement

K.P. Wyche: Conceptualization, Data curation, Formal analysis, Funding acquisition, Investigation, Methodology, Project administration, Resources, Software, Supervision, Validation, Visualization, Writing - original draft, Writing - review & editing. **M. Nichols:** Conceptualization, Data curation, Formal analysis, Investigation, Methodology, Project administration, Resources, Validation, Visualization, Writing - original draft, Writing - review & editing. **H. Parfitt:** Conceptualization, Data curation, Formal analysis, Investigation, Methodology, Resources, Software, Validation, Visualization, Writing - review & editing. **P. Beckett:** Funding acquisition, Investigation, Supervision, Validation, Writing - review & editing. **D.J. Gregg:** Data curation, Formal analysis, Investigation, Methodology, Software, Validation, Visualization, Writing - review & editing. **K.L. Smallbone:** Funding acquisition, Investigation, Supervision, Validation, Writing - review & editing. **P.S. Monks:** Funding acquisition, Investigation, Supervision, Validation, Writing - review & editing.

Declaration of competing interest

The authors declare that they have no known competing financial interests or personal relationships that could have appeared to influence the work reported in this paper.

Acknowledgements

This study was conducted as part of the *Hidden Rise In Toxic Air Pollution (HRITAP)* project, funded by the Natural Environment Research Council (NERC) as part of UK Research and Innovation's (UKRI) rapid response to COVID-19 (grant reference number: NE/V009400/1). The *JOAQUIN Advanced Atmospheric reSearch* laboratory was funded as part of the *Joint Air Quality Initiative (JOAQUIN)* project by the INTERREG IVB North West Europe programme (www.nweurope.eu) and the University of Brighton. Data from the AURN was provided courtesy of the UK Department for Food and Rural Affairs (DEFRA) and data from the Sussex-Air Network was provided courtesy of the Sussex-Air partnership. The authors also acknowledge the TROPOMI mission scientists and associated Sentinel-5P personnel for the production of the TROPOMI data used herein. The authors would like to thank Dr. Hannah Wood for assistance with preparing figures for publication.

Appendix A. Supplementary data

Supplementary data to this article can be found online at <https://doi.org/10.1016/j.scitotenv.2020.142526>.

References

- Aliche, B., Platt, U. & Stutz, J. 2002. Impact of nitrous acid photolysis on the total hydroxyl radical budget during the Limitation of Oxidant Production/Pianura Padana Produzione di Ozono study in Milan. *Journal of Geophysical Research: Atmospheres*, 107, LOP 9-1-LOP 9-17.
- Alipio, M., 2020. Do latitude and ozone concentration predict Covid-2019 cases in 34 countries? Available at SSRN 3572114.
- AQEG 2004. Nitrogen Dioxide in the UK [Online]. UK: Air Quality Expert Group. Available: <https://uk-air.defra.gov.uk/library/assets/documents/reports/aeq/nd-chapter2.pdf> [Accessed 2020].
- AQEG 2009. Ozone in the United Kingdom. UK: Air Quality Expert Group. Available: <https://uk-air.defra.gov.uk/assets/documents/reports/aeq/aeq-ozone-report.pdf> [Accessed 2020].
- AQEG 2012. Fine Particulate Matter (PM_{2.5}) in the United Kingdom [online]. UK: Air Quality Expert Group. Available: https://uk-air.defra.gov.uk/assets/documents/reports/cat1/1212141150_AQEG_Fine_Part particulate_Matter_in_the_UK.pdf [Accessed 2020].

- AQEG, 2020a. Estimation of changes in air pollution emissions, concentrations and exposure during the COVID-19 outbreak in the UK. Rapid Evidence Review – June 2020. Air Quality Expert Group, UK https://uk-air.defra.gov.uk/assets/documents/reports/cat09/2007010844_Estimation_of_Changes_in_Air_Pollution_During_COVID-19_outbreak_in_the_UK.pdf.
- AQEG, 2020b. Annex to the AQEG Report - Submissions Cited in the Published Work: Estimation of Changes in Air Pollution Emissions, Concentrations and Exposure during the COVID-19 Outbreak in the UK. Air Quality Expert Group, UK.
- Araujo, J.A., Nel, A.E., 2009. Particulate matter and atherosclerosis: role of particle size, composition and oxidative stress. *Particle and fibre toxicology* 6, 24.
- Atkinson, R., 2000. Atmospheric chemistry of VOCs and NOx. *Atmos. Environ.* 34, 2063–2101.
- Brocco, D., Fratarcangeli, R., Lepore, L., Petricca, M., Ventrone, I., 1997. Determination of aromatic hydrocarbons in urban air of Rome. *Atmos. Environ.* 31, 557–566.
- Calvert, J.G., Kerr, J.A., Demerjian, K.L., McQuigg, R.D., 1972. Photolysis of formaldehyde as a hydrogen atom source in the lower atmosphere. *Science* 175, 751–752.
- Calvert, J., Yarwood, G., Dunker, A., 1994. An evaluation of the mechanism of nitrous acid formation in the urban atmosphere. *Res. Chem. Intermed.* 20, 463–502.
- Calvert, J.G., Atkinson, R., Becker, K.H., Kamens, R.M., Seinfeld, J.H., Wallington, T.H., Yarwood, G., 2002. *The Mechanisms of Atmospheric Oxidation of the Aromatic Hydrocarbons*. Oxford University Press.
- Calvert, J.G., Derwent, R.G., Orlando, J.J., Wallington, T.J., Tyndall, G.S., 2008. *Mechanisms of Atmospheric Oxidation of the Alkanes* (OUP USA).
- Carlsaw, D. 2015. The openair manual open-source tools for analysing air pollution data [Online]. Available: http://www.openair-project.org/PDF/OpenAir_Manual.pdf [Accessed 2020].
- Carlsaw, D. 2020. Import Surface Meteorological Data from NOAA Integrated Surface Database (ISD) [online]. RDocumentation. Available: <https://www.rdocumentation.org/packages/worldmet/versions/0.8.8> [Accessed 2020].
- Chen, Q.X., Huang, C.L., Yuan, Y. and Tan, H.P., Influence of COVID-19 Event on Air Quality and their Association in Mainland China. *Aerosol and Air Quality Research*, 2020.
- Cole, M., Ozgen, C., Strobl, E., 2020. Air Pollution Exposure and COVID-19, IZA Discussion Paper No. 13367, Available at SSRN. <https://ssrn.com/abstract=3628242>.
- Comunian, S., Dongo, D., Milani, C., Palestini, P., 2020. Air pollution and Covid-19: the role of particulate matter in the spread and increase of covid-19's morbidity and mortality. *International Journal of Environmental Research and Public Health* 17 (12), 4487.
- COPERNICUS. 2020. Sentinel-5P Pre-operations Data Hub [Online]. European Space Agency. Available: <https://s5phub.copernicus.eu/dhus/#/home> [Accessed 2020].
- Cordell, R., Mazet, M., Dechoux, C., Hama, S., Staelens, J., Hofman, J., Stroobants, C., Roekens, E., Kos, G., Weijers, E., 2016. Evaluation of biomass burning across North West Europe and its impact on air quality. *Atmos. Environ.* 141, 276–286.
- Correa, S.M., Arbilla, G., 2006. Aromatic hydrocarbons emissions in diesel and biodiesel exhaust. *Atmos. Environ.* 40, 6821–6826.
- Crapo, J.D., Barry, B.E., Chang, L.Y., Mercer, R.R., 1984. Alterations in lung structure caused by inhalation of oxidants. *Journal of Toxicology and Environmental Health, Part A Current Issues* 13, 301–321.
- DEFRA, 2017. UK Plan for Tackling Roadside Nitrogen Dioxide Concentrations. An Overview. Department for Food and Rural Affairs, UK.
- DEFRA. 2020a. Automatic Urban and Rural Network (AURN) [Online]. UK Government Department for Food and Rural Affairs. Available: <https://uk-air.defra.gov.uk/networks/network-info?view=aur> [Accessed 08/07/2020].
- DEFRA. 2020b. National Statistics Emissions of air pollutants in the UK, 1970 to 2018 – Nitrogen oxides (NOx) [Online]. UK: Department for Food and Rural Affairs. Available: <https://www.gov.uk/government/publications/emissions-of-air-pollutants/annual-emissions-of-nitrogen-oxides-in-the-uk-1970-2018#:~:text=Emissions%20of%20nitrogen%20oxides%20have,year%20between%201990%20and%202018.> [Accessed 2020].
- DFT. 2020. Official Statistics. Transport Use During the Coronavirus (COVID-19) Pandemic [Online]. UK: Department for Transport. Available: <https://www.gov.uk/government/statistics/transport-use-during-the-coronavirus-covid-19-pandemic> [Accessed 2020].
- ECDC 2020. COVID-19 Situation Update Worldwide, as of 10 July 2020 [Online]. European Centre for Disease Prevention and Control. Available: <https://www.ecdc.europa.eu/en/geographical-distribution-2019-ncov-cases> [Accessed 2020].
- Eskes, H. J., VAN Gaffen, J., Boersma, K. F., Eichmann, K.-U., Apituley, A., Pedergnana, S., Veeffkind, J. P. & Loyola, D. 2019. Sentinel-5 precursor/TROPOMI Level 2 Product User Manual Nitrogen Dioxide. [Online]. Netherlands: Royal Netherlands Meteorological Institute. Available: <https://sentinel.esa.int/documents/247904/2474726/Sentinel-5P-Level-2-Product-User-Manual-Nitrogen-Dioxide> [Accessed 2020].
- Finlayson-Pitts, B., Pitts Jr., J., 1993. Atmospheric chemistry of tropospheric ozone formation: scientific and regulatory implications. *Air Waste* 43, 1091–1100.
- Finlayson-Pitts, B., Wingen, L., Sumner, A., Syomin, D., Ramazan, K., 2003. The heterogeneous hydrolysis of NO₂ in laboratory systems and in outdoor and indoor atmospheres: an integrated mechanism. *Phys. Chem. Chem. Phys.* 5, 223–242.
- Franco, B., Marais, E.A., Bovy, B., Bader, W., Lejeune, B., Roland, G., Servais, C., Mahieu, E., 2016. Diurnal cycle and multi-decadal trend of formaldehyde in the remote atmosphere near 46° N. *Atmos. Chem. Phys.* 16, 4171–4189.
- Fried, A., Mckeen, S., Sewell, S., Harder, J., Henry, B., Goldan, P., Kuster, W., Williams, E., Baumann, K., Shetter, R., 1997. Photochemistry of formaldehyde during the 1993 Tropospheric OH Photochemistry Experiment. *Journal of Geophysical Research: Atmospheres* 102, 6283–6296.
- Fu, X., Wang, T., Zhang, L., Li, Q., Wang, Z., Xia, M., Yun, H., Wang, W., Yu, C., Yue, D., 2019. The Significant Contribution of HONO to Secondary Pollutants during a Severe Winter Pollution Event in Southern China.
- Grange, S.K., Carlsaw, D.C., 2019. Using meteorological normalisation to detect interventions in air quality time series. *Sci. Total Environ.* 653, 578–588.
- Greenstone, M., Fan, C.Q., 2018. *Introducing the air quality life index. Twelve Facts about Particulate Air Pollution, Human Health, and Global Policy*. University of Chicago, Energy Policy Institute.
- Guo, S., Hu, M., Peng, J., Wu, Z., Zamora, M.L., Shang, D., Du, Z., Zheng, J., Fang, X., Tang, R., 2020. Remarkable nucleation and growth of ultrafine particles from vehicular exhaust. *Proceedings of the National Academy of Sciences* 117, 3427–3432.
- Haagen-Smit, A.J., Fox, M., 1954. Photochemical ozone formation with hydrocarbons and automobile exhaust. *Air Repair* 4, 105–136.
- Harris, G.W., Carter, W.P., Winer, A.M., Pitts, J.N., Platt, U., Perner, D., 1982. Observations of nitrous acid in the Los Angeles atmosphere and implications for predictions of ozone-precursor relationships. *Environmental science & technology* 16, 414–419.
- Harrison, R.M., Yin, J., 2000. Particulate matter in the atmosphere: which particle properties are important for its effects on health? *Sci. Total Environ.* 249, 85–101.
- Harrison, R.M., Peak, J.D., Collins, G.M., 1996. Tropospheric cycle of nitrous acid. *Journal of Geophysical Research: Atmospheres* 101, 14429–14439.
- Hofman, J., Staelens, J., Cordell, R., Stroobants, C., Zikova, N., Hama, S., Wyche, K., Kos, G., van der Zee, S., Smallbone, K., 2016. Ultrafine particles in four European urban environments: results from a new continuous long-term monitoring network. *Atmos. Environ.* 136, 68–81.
- Jenkin, M.E., Saunders, S.M., Pilling, M.J., 1997. The tropospheric degradation of volatile organic compounds: a protocol for mechanism development. *Atmos. Environ.* 31, 81–104.
- Jenkin, M., Saunders, S., Wagner, V., Pilling, M., 2002. Protocol for the Development of the Master Chemical Mechanism, MCM v3 (Part B): Tropospheric Degradation of Aromatic Volatile Organic Compounds.
- Ju, M.J., Oh, J., Choi, Y.H., 2020. Changes in air pollution levels after COVID-19 outbreak in Korea. *Science of the Total Environment*, p. 141521.
- Kerbachi, R., Boughedaoui, M., Bounoua, L., Keddad, M., 2006. Ambient air pollution by aromatic hydrocarbons in Algiers. *Atmos. Environ.* 40, 3995–4003.
- Kerimray, A., Baimatova, N., Ibragimova, O.P., Bukenov, B., Kenessov, B., Plotitsyn, P., Karaca, F., 2020. Assessing air quality changes in large cities during COVID-19 lockdowns: the impacts of traffic-free urban conditions in Almaty, Kazakhstan. *Science of the Total Environment* 139179.
- Kirchstetter, T.W., Harley, R.A., Littlejohn, D., 1996. Measurement of nitrous acid in motor vehicle exhaust. *Environmental science & technology* 30, 2843–2849.
- Kleinman, L.L., 1994. Low and high NOx tropospheric photochemistry. *Journal of Geophysical Research: Atmospheres* 99, 16831–16838.
- Le, T., Wang, Y., Liu, L., Yang, J., Yung, Y.L., Li, G., Seinfeld, J.H., 2020. Unexpected air pollution with marked emission reductions during the COVID-19 outbreak in China. *Science* 369 (6504), 702–706.
- Lee, M., Heikes, B.G., O'sullivan, D.W., 2000. Hydrogen peroxide and organic hydroperoxide in the troposphere: a review. *Atmos. Environ.* 34, 3475–3494.
- Lelieveld, J., Dentener, F.J., 2000. What controls tropospheric ozone? *Journal of Geophysical Research: Atmospheres* 105, 3531–3551.
- Levy, H., 1971. Normal atmosphere: large radical and formaldehyde concentrations predicted. *Science* 173, 141–143.
- Liu, F., Beirle, S., Zhang, Q., Dörner, S., He, K., Wagner, T., 2016. NOx lifetimes and emissions of cities and power plants in polluted background estimated by satellite observations. *Atmos. Chem. Phys.* 16, 5283.
- Madronich, S., 1993. Tropospheric photochemistry and its response to UV changes. Springer, *The Role of the Stratosphere in Global Change*.
- Manoj, M.G., Kumar, M.S., Valsaraj, K.T., Sivan, C., Vijayan, S.K., 2020. Potential link between compromised air quality and transmission of the novel corona virus (SARS-CoV-2) in affected areas. *Environmental Research*, p. 110001.
- Marnar, B., Laxen, D., Gellatly, R., Liska, T., 2020. Response to AQEG Request for Rapid Evidence on COVID-19 & UK Air Quality (Air Quality Consultants).
- Melkonyan, A., Kuttler, W., 2012. Long-term analysis of NO, NO₂ and O₃ concentrations in North Rhine-Westphalia, Germany. *Atmos. Environ.* 60, 316–326.
- Monks, P.S., 2005. Gas-phase radical chemistry in the troposphere. *Chem. Soc. Rev.* 34, 376–395.
- Monks, P. S. 2020. Coronavirus: lockdown's effect on air pollution provides rare glimpse of low-carbon future [online]. *The Conversation*. Available: <https://theconversation.com/coronavirus-lockdowns-effect-on-air-pollution-provides-rare-glimpse-of-low-carbon-future-134685> [Accessed 2020].
- Monks, P.S., Archibald, A., Colette, A., Cooper, O., Coyle, M., Derwent, R., Fowler, D., Granier, C., Law, K.S., Mills, G., 2015. Tropospheric Ozone and Its Precursors From the Urban to the Global Scale From Air Quality to Short-lived Climate Forcer.
- Munn, R.E., 1981. *Design of Air Quality Monitoring Networks*. Springer.
- Mustafa, M.G., Elsayed, N.M., VON Dohlen, F.M., Hassett, C.M., Postlethwait, E.M., Quinn, C.L., Graham, J.A., Gardner, D.E., 1984. A comparison of biochemical effects of nitrogen dioxide, ozone, and their combination in mouse lung: I. Intermittent exposures. *Toxicology and applied pharmacology* 72, 82–90.
- Myllyvirta, L., Thieriot, H., 2020. 11,000 Air Pollution-related Deaths Avoided in Europe as Coal, Oil Consumption Plummet (Centre for Research on Energy and Clean Air).
- NAEI. 2019a. Pollutant Information: Nitrogen Oxides [Online]. National Atmospheric Emissions Inventory. Available: https://naei.beis.gov.uk/overview/pollutants?pollutant_id=6 [Accessed 2020].
- NAEI. 2019b. Pollutant Information: Non Methane VOC [Online]. National Atmospheric Emissions Inventory. Available: https://naei.beis.gov.uk/overview/pollutants?pollutant_id=9 [Accessed 2020].
- NASA, 2020. NASA, ESA, JAXA Release Global View of COVID-19 Impacts [Online]. Goddard Media Studios Available. <https://svs.gsfc.nasa.gov/13647> (Accessed).
- ONS. 2020. Census Output Area population estimates – South East, England (supporting information) [Online]. Office for National Statistics. Available: <https://www.ons.gov.uk/peoplepopulationandcommunity/populationandmigration/populationestimates/datasets/censusoutputareastimatesinthesoutheastregionofengland> [Accessed].

- Parrish, D., Ryerson, T., Mellqvist, J., Johansson, J., Fried, A., Richter, D., Walega, J., Washenfelder, R.D., DE Gouw, J., Peischl, J., 2012. Primary and secondary sources of formaldehyde in urban atmospheres: Houston Texas region. *Atmos. Chem. Phys.* 12, 3273–3288.
- PHE. 2020a. Coronavirus (COVID-19) in the UK [Online]. Public Health England. Available: <https://coronavirus.data.gov.uk/> [Accessed 07/07/2020 2020].
- PHE, 2020b. The Health Protection (Coronavirus, Restrictions) (England) Regulations 2020. Public Health England.
- Pope, F.D., Smith, C.A., Davis, P.R., Shallcross, D.E., Ashfold, M.N., Orr-Ewing, A.J., 2005. Photochemistry of formaldehyde under tropospheric conditions. *Faraday Discuss.* 130, 59–72.
- Pun, B.K., Seigneur, C., White, W., 2003. Day-of-week behavior of atmospheric ozone in three US cities. *J. Air Waste Manage. Assoc.* 53, 789–801.
- Roberts-Semple, D., Song, F., Gao, Y., 2012. Seasonal characteristics of ambient nitrogen oxides and ground-level ozone in metropolitan northeastern New Jersey. *Atmospheric Pollution Research* 3, 247–257.
- Rückerl, R., Schneider, A., Breitner, S., Cyrus, J., Peters, A., 2011. Health effects of particulate air pollution: a review of epidemiological evidence. *Inhal. Toxicol.* 23, 555–592.
- Rutz, C., Loretto, M.-C., Bates, A.E., Davidson, S.C., Duarte, C.M., Jetz, W., Johnson, M., Kato, A., Kays, R., Mueller, T., 2020. COVID-19 lockdown allows researchers to quantify the effects of human activity on wildlife. *Nature Ecology & Evolution* 1–4.
- Rychlik, K.A., Secrest, J.R., Lau, C., Pulczynski, J., Zamora, M.L., Leal, J., Langley, R., Myatt, L.G., Raju, M., Chang, R.C.-A., 2019. In utero ultrafine particulate matter exposure causes offspring pulmonary immunosuppression. *Proceedings of the National Academy of Sciences* 116, 3443–3448.
- Salisbury, G., Monks, P., Bauguitte, S., Bandy, B., Penkett, S., 2002. A seasonal comparison of the ozone photochemistry in clean and polluted air masses at Mace Head, Ireland. *J. Atmos. Chem.* 41, 163–187.
- Saunders, S.M., Jenkin, M.E., Derwent, R., Pilling, M., 2003. Protocol for the Development of the Master Chemical Mechanism, MCM v3 (Part A): Tropospheric Degradation of Non-aromatic Volatile Organic Compounds.
- Setti, L., Passarini, F., De Gennaro, G., Barbieri, P., Perrone, M.G., Borelli, M., Palmisani, J., Di Gilio, A., Torboli, V., Fontana, F., Clemente, L., 2020. SARS-Cov-2RNA Found on Particulate Matter of Bergamo in Northern Italy: First Evidence. *Environmental Research*, p. 109754.
- Sharma, S., Zhang, M., Gao, J., Zhang, H., Kota, S.H., 2020. Effect of restricted emissions during COVID-19 on air quality in India. *Sci. Total Environ.* 728, 138878.
- Sicard, P., DE Marco, A., Agathokleous, E., Feng, Z., Xu, X., Paoletti, E., Rodriguez, J.J.D., Calatayud, V., 2020. Amplified ozone pollution in cities during the COVID-19 lockdown. *Science of The Total Environment* 735, 139542 <https://dx.doi.org/10.1016%2Fj.scitotenv.2020.139542>.
- Siciliano, B., Dantas, G., DA Silva, C.M., Arbilla, G., 2020. Increased ozone levels during the COVID-19 lockdown: analysis for the city of Rio de Janeiro, Brazil. *Science of The Total Environment* 737, 139765 <https://dx.doi.org/10.1016%2Fj.scitotenv.2020.139765>.
- Sillman, S., 1999. The relation between ozone, NOx and hydrocarbons in urban and polluted rural environments. *Atmos. Environ.* 33, 1821–1845.
- SUSSEX-AIR. 2020. *Sussex-Air* [Online]. Available: <http://www.sussex-air.net/> [Accessed].
- Team, R. D. C. 2015. R: A Language and Environment for Statistical Computing. R Foundation for Statistical Computing, R Development Core Team, Vienna, Austria.
- Tobías, A., Carnerero, C., Reche, C., Massagué, J., Via, M., Minguillón, M.C., Alastuey, A., Querol, X., 2020. Changes in air quality during the lockdown in Barcelona (Spain) one month into the SARS-CoV-2 epidemic. *Sci. Total Environ.* 138540.
- Travaglio, M., Yu, Y., Popovic, R., Leal, N.S., Martins, L.M., 2020. Links between air pollution and COVID-19 in England. *medRxiv*.
- Tung, N.T., Cheng, P.C., Chi, K.H., Hsiao, T.C., Jones, T., Bérubé, K., Ho, K.F., Chuang, H.C., 2020. Particulate matter and SARS-CoV-2: a possible model of COVID-19 transmission. *Science of The Total Environment*, p. 141532.
- Wenig, M., Spichtinger, N., Stohl, A., Held, G., Beirle, S., Wagner, T., Jähne, B., Platt, U., 2003. Intercontinental Transport of Nitrogen Oxide Pollution Plumes.
- WHO, 2016. Ambient Air Pollution: A Global Assessment of Exposure and Burden of Disease (World Health Organisation).
- WHO. 2018. 9 out of 10 people worldwide breathe polluted air, but more countries are taking action [Online]. Geneva. Available: <https://www.who.int/news-room/detail/02-05-2018-9-out-of-10-people-worldwide-breathe-polluted-air-but-more-countries-are-taking-action> [Accessed].
- Wolff, G.T., Korsog, P.E., 1992. Ozone control strategies based on the ratio of volatile organic compounds to nitrogen oxides. *J. Air Waste Manage. Assoc.* 42, 1173–1177.
- Wu, X., Nethery, R.C., Sabath, B.M., Braun, D., Dominici, F., 2020. Exposure to air pollution and COVID-19 mortality in the United States. *medRxiv*. <https://doi.org/10.1101/2020.04.05.20054502>.
- Wyche, K.P., Cordell, R.L., L. Smith, M., Smallbone, K.L., Lyons, P., Hama, S.M.L., Monks, P.S., Staelens, J., Hofman, J., Stroobants, C., Roekens, E., Kos, G.P.A., Weijers, E.P., Panteliadis, P., Dijkema, M.B.A., 2020. The spatio-temporal evolution of black carbon in the North-West European 'air pollution' hotspot. *Atmospheric Environment, At Review*.
- Yang, Y., Shao, M., Wang, X., Nölscher, A.C., Kessel, S., Guenther, A., Williams, J., 2016. Towards a quantitative understanding of total OH reactivity: a review. *Atmos. Environ.* 134, 147–161.
- Zangari, S., Hill, D.T., Charette, A.T., Mirowsky, J.E., 2020. Air quality changes in New York City during the COVID-19 pandemic. *Sci. Total Environ.* 742, 140496.
- Zhang, J., Wei, Y., Fang, Z.F., 2019. Ozone pollution: a major health hazard worldwide. *Front. Immunol.* 10, 2518.
- Zhang, J., Cui, K., Wang, Y.F., Wu, J.L., Huang, W.S., Wan, S., Xu, K., 2020. Temporal variations in the air quality index and the impact of the COVID-19 event on air quality in Western China. *Aerosol Air Qual. Res.* 20.